Contents lists available at ScienceDirect

NeuroImage

journal homepage: www.elsevier.com/locate/neuroimage

Original Research

Neural substrates of human fear generalization: A 7T-fMRI investigation

Ashley A. Huggins [a,1], Carissa N. Weis [a], Elizabeth A. Parisi [a], Kenneth P. Bennett [b], Vladimir Miskovic [c], Christine L. Larson [a,*]

[a] University of Wisconsin – Milwaukee, Department of Psychology, Milwaukee, WI, United States
[b] Montana VA Healthcare System, Helena, MT, United States
[c] Binghamton University, Department of Psychology, Binghamton, NY United States

A B S T R A C T

Fear generalization - the tendency to interpret ambiguous stimuli as threatening due to perceptual similarity to a learned threat – is an adaptive process. Overgeneralization, however, is maladaptive and has been implicated in a number of anxiety disorders. Neuroimaging research has indicated several regions sensitive to effects of generalization, including regions involved in fear excitation (e.g., amygdala, insula) and inhibition (e.g., ventromedial prefrontal cortex). Research has suggested several other small brain regions may play an important role in this process (e.g., hippocampal subfields, bed nucleus of the stria terminalis [BNST], habenula), but, to date, these regions have not been examined during fear generalization due to limited spatial resolution of standard human neuroimaging. To this end, we utilized the high spatial resolution of 7T fMRI to characterize the neural circuits involved in threat discrimination and generalization. Additionally, we examined potential modulating effects of trait anxiety and intolerance of uncertainty on neural activation during threat generalization. In a sample of 31 healthy undergraduate students, significant positive generalization effects (i.e., greater activation for stimuli with increasing perceptual similarity to a learned threat cue) were observed in the visual cortex, thalamus, habenula and BNST, while negative generalization effects were observed in the dentate gyrus, CA1, and CA3. Associations with individual differences were underpowered, though preliminary findings suggested greater generalization in the insula and primary somatosensory cortex may be correlated with self-reported anxiety. Overall, findings largely support previous neuroimaging work on fear generalization and provide additional insight into the contributions of several previously unexplored brain regions.

1. Introduction

Fear generalization is an adaptive process that enables an organism to respond appropriately to novel, possibly harmful, stimuli based on the presence of perceptual features that are similar to a learned threat cue. However, this process can prove maladaptive when individuals *over*generalize and exhibit fear responding to environmental cues that actually signal safety. Overgeneralization of fear has oft been neglected scientifically in human studies (Dymond et al., 2015); however, it has profound clinical significance and is implicated in the pathophysiology of several psychiatric disorders, including anxiety and posttraumatic stress disorder (PTSD; Lissek et al., 2008, 2014b, 2009; Morey et al., 2015). A better understanding of the complexities of fear generalization and the neural circuitry instantiating the behavior is likely to provide important insight into the pathophysiology of these disorders and potentially aid in the development of novel treatment targets.

Emerging research has shed light on the basic neural processes supporting fear generalization. Experimental paradigms typically utilize a Pavlovian conditioning design to condition participants to an initially neutral cue (conditioned stimulus; CS+) by presenting it with a naturally aversive stimulus (unconditioned stimulus; US), such as electric shock. After conditioning, a series of generalization stimuli (GSs) that parametrically vary in perceptual overlap with the CS+ are introduced (Dunsmoor et al., 2009; Lissek et al., 2008). Generalization gradients tracking behavioral and psychophysiological responses across stimuli varying in perceptual similarity generally depict robust fear responding to the CS+, with a fairly steep, quadratic decline as GSs become increasingly dissimilar, reflecting an appropriate balance of excitatory versus inhibitory processes (Asok et al., 2019; Dunsmoor et al., 2009, 2011; Lissek et al., 2014a). However, when overgeneralization occurs, these gradients assume a more linear or convex shape, indicating safe GSs are perceived as threatening.

Neuroimaging research has elucidated a number of distinct brain regions sensitive to effects of generalization. Regions including the insula, dorsal anterior cingulate cortex (dACC), thalamus, periaqueductal grey (PAG), caudate, and ventral tegmental area (VTA) demonstrate positive generalization gradients, wherein neural activation increases with increasing similarity to threat; in contrast, the hippocampus, ventromedial prefrontal cortex (vmPFC) and precuneus demonstrate negative generalization gradients, wherein activation *de*creases with increasing similarity to threat (Dunsmoor et al., 2009; Lissek et al., 2014b; Spalding, 2018). That said, many of the brain regions implicated in the process of fear generalization are heterogeneous in nature and relatively large in size; as such, there may be important structural and/or functional subdivisions that differentially contribute to threat generalization (Fox et al., 2015; Strange et al., 1999; Zimmerman et al., 2007). In particular, extant research suggests the hippocampal subfields, amygdala subnuclei, and habenula are functionally relevant to fear generalization, but they have not been typically examined in this literature as their small size makes it difficult to characterize their contributions with standard neuroimaging parameters.

Broadly, the hippocampus is proposed to play a critical role in fear generalization. Indeed, lesions of the hippocampus and its cortical inputs increase threat generalization (Bucci et al., 2002; Solomon and Moore, 1975; Wild and Blampied, 1972). Neural models of generalization are largely grounded in the hippocampus (e.g., Lissek, 2012), based on hippocampal-dependent processes subserving stimulus discrimination via pattern separation and completion (McHugh et al., 2007; Rolls, 2013; Yassa and Stark, 2011). In the context of incomplete or ambiguous sensory information, sufficient overlap between a novel stimulus and learned threat cue leads to pattern completion in the hippocampus and subsequent engagement of structures involved in fear excitation (e.g., amygdala, insula); however, if neural representations of these stimuli are more distinct, the hippocampus initiates pattern separation and recruits structures involved in fear inhibition (e.g., vmPFC; (Lissek, 2012)).

Importantly, pattern separation and completion processes are attributed to different subfields of the hippocampus (McHugh et al., 2007; Rolls, 2013; Yassa and Stark, 2011). Animal research has provided strong evidence for the dentate gyrus facilitating pattern separation, which is perhaps supported by neurogenesis within this region (Amaral et al., 2007; Clelland et al., 2009; Glover et al., 2017). Although research examining dentate gyrus function in humans is relatively scarce – largely limited by difficulties in clearly defining spatial boundaries of hippocampal subfields - emerging research has demonstrated a bias toward pattern separation in the dentate gyrus/CA3 subfield, while the CA1 subfield is biased toward pattern completion (Bakker et al., 2008; Dimsdale-Zucker et al., 2018; Lacy et al., 2011).

Theoretically, the amygdala is also thought to play a significant role in threat generalization; yet, despite a rich history of research that has well-documented the region's role in the detection and regulation of threat responding (Davis, 1992; LeDoux, 2003), the amygdala is inconsistently implicated in fear generalization (Dunsmoor et al., 2011; Kaczkurkin et al., 2017; Lissek et al., 2014a), as well as human fear conditioning more generally (see Fullana et al. (2016) for meta-analytic work). This inconsistency perhaps relates to functional divergence across amygdala subnuclei. Notably, within the amygdala, the lateral nucleus (LA) has been proposed as a key site of plasticity for fear learning and memory (Goosens and Maren, 2001). Sensory information via thalamic relay nuclei is received by the basolateral amygdala (BLA) where it is integrated with contextual information that helps to establish threat contingencies. This information is then transmitted to the central amygdala (CeA) along with other regions, such as the striatum, to mediate adaptive behaviors (e.g., fight-or-flight response; Janak and Tye, 2015). The amygdala shares strong anatomical and functional connections with the bed nucleus of the stria terminalis (BNST; Avery et al., 2014; Torrisi et al., 2015), an understudied region also implicated in threat responding (Davis et al., 2010; Lebow and Chen, 2016). Together

with the CeA, the BNST is considered part of an anatomically defined macrostructure of several small, tightly interconnected regions referred to as the extended amygdala (Shackman and Fox, 2016; Tyszka and Pauli, 2016). While the CeA is thought to mediate more immediate, phasic responding to an identifiable threat (i.e., 'fear'), the amygdala's lateral nuclei and BNST are thought to support more sustained apprehensive states (i.e., 'anxiety'; Davis et al., 2010; Klumpers et al., 2017; but see also Hur et al., 2020; Shackman and Fox, 2016).

These distinct subregions may differentially contribute to threat generalization. For instance, animal research suggests the BLA is prone to generalization when stimuli are associated with threat (Grosso et al., 2018; Resnik and Paz, 2015). The BNST may also be sensitive to threat generalization, playing a key role in processing ambiguous and/or unpredictable threat cues (Alvarez et al., 2011; Goode et al., 2019; Somerville et al., 2010). Functional connectivity studies have shown overlapping and distinct functional connections of the BNST and amygdala subnuclei (Gorka et al., 2018; Tillman et al., 2018; Torrisi et al., 2015, 2018; Weis et al., 2019). The amygdala's role in fear generalization remains unclear, thus considering the broader amygdaloid complex and its subdivisions may provide clarification. For instance, ambiguity related to the shared perceptual features between a novel stimulus and a conditioned threat cue may drive BNST activation during generalization, while increased generalization may be observed uniquely in the BLA.

The habenula, a region proposed to play a pivotal role in enabling adaptive behavior related to both threat and reward, may also play a key role in generalization. The habenula serves as an important interface between core affective regions and the brainstem (Boulos et al., 2017; Epstein et al., 2018), and has critical structural and functional connections with the medial prefrontal cortex, ACC, and hippocampus (Ely et al., 2016; Shelton et al., 2012; Torrisi et al., 2017). Researchers have proposed that the habenula's chief role is in signaling the occurrence of negative events and integrating information about internal states and external context in order to modulate or adapt behavior (Boulos et al., 2017; Epstein et al., 2018; Salas et al., 2010). Neuronal recordings from the habenula have demonstrated increased activity in response to behaviorally salient negative events, such as threat cues (Hikosaka, 2010; Durieux et al., 2020; Matsumoto and Hikosaka, 2007). In humans, habenula activation is observed in response to conditioned threat cues (Hennigan et al., 2015; Lawson et al., 2017). Thus, the habenula may play a role in integrating information about a learned threat in order to flexibly respond (i.e., by either generalizing or discriminating between stimuli). However, measuring only about 15–36 mm^3 in volume in humans (Lawson et al., 2013), there is very little research on habenular function in humans.

From a translational perspective, a more granular functional mapping of these brain regions during threat generalization may have substantial clinical implications. While fear generalization is an adaptive process, evidence suggests this process goes awry in anxiety disorders and becomes maladaptive, such that individuals respond fearfully to cues that actually confer safety (Dymond et al., 2015; Lissek, 2012). Clinical observations clearly illustrate how this overexpression of fear in the context of safety can cause profound distress and impairment in an individual's daily functioning. For example, an assaultive trauma survivor may experience intense distress when triggered by seeing someone who resembles their attacker. Overgeneralized fear may also contribute to avoidance of activities that provide positive reinforcement or are instrumental to daily living (e.g., avoiding driving after a motor vehicle accident). Overgeneralization of fear is seen across a number of anxiety-related pathologies, including panic (Lissek et al., 2009), generalized anxiety (Cha et al., 2014; Lissek et al., 2014b), social anxiety (Ahrens et al., 2016; (Stegmann et al., 2020) and posttraumatic stress disorders (Lis et al., 2020; Lissek and van Meurs, 2015; Thome et al., 2018). Neuroimaging in clinical samples is limited but implicate aberrant activation of regions such as the insula, hippocampus, vmPFC, and caudate in PTSD (Kaczkurkin et al., 2017; Morey et al., 2015) and gener-

alized anxiety disorder (Cha et al., 2014; Greenberg et al., 2013) during fear generalization.

More broadly, anxious pathology has been frequently associated with disrupted function in brain regions relevant to fear generalization, such as the insula, amygdala, and vmPFC (Etkin and Wager, 2007). Moreover, there appear to be unique aberrancies in several of these small regions and subregions. For instance, reduced dentate gyrus and CA3 volume may help explain overgeneralization in clinical samples (Hayes et al., 2017; Wang et al., 2010), and impaired pattern separation (as well as deficient neurogenesis in the dentate gyrus) has been proposed as an endophenotype for anxiety disorders (Besnard and Sahay, 2016; Kheirbek et al., 2012). Specifically, a pattern completion bias may lead anxious individuals to overgeneralize new information to fit an existing representation of threat. Regarding the amygdala, altered functional connectivity of the BLA, but not CeA, differentiates PTSD patients from trauma-exposed controls (Brown et al., 2014). Generalized anxiety disorder is associated with greater BNST activation during conditions of uncertainty (Yassa et al., 2012). Hyperactivation of the habenula has been related to anxiety and defensive responding in rats and zebrafish (Mathuru and Jesuthasan, 2013; Pobbe and Zangrossi, 2008); though limited, emerging human research suggests habenular dysfunction is observed in depression, which is highly comorbid with anxiety (Lawson et al., 2017; Yoshino et al., 2018). Together, these findings warrant further examination of how these regions function during fear generalization to better map brain and behavior onto clinical phenotypes.

It is also important to consider how *non*-clinical levels of anxiety may modulate fear generalization. Most research to date has focused on examining generalization between patient and control populations, rather than focusing on individual difference factors. Several studies have examined generalization as related to trait anxiety, although findings have been somewhat inconsistent; some studies have suggested trait anxiety is related to overgeneralization (Haddad et al., 2013; Wong and Lovibond, 2018), while others have failed to find an association (Arnaudova et al., 2017; Torrents-Rodas et al., 2013).

To this end, it is important to examine anxiety-relevant transdiagnostic constructs that may more specifically encapsulate the cognitive processes playing into fear generalization. Intolerance of uncertainty - the extent to which an individual experiences distress or anxiety in response to unpredictable or ambiguous information – may contribute to excessive worry and anxiety when discriminating threat and lead to fear generalization (Buhr and Dugas, 2002; Ladouceur et al., 2000). Intolerance of uncertainty has been extensively implicated in the etiology and maintenance of anxiety (Correa et al., 2019; Dugas et al., 1998; Osmanağaoğlu et al., 2018; Shihata et al., 2016). Moreover, higher intolerance of uncertainty has been shown to be uniquely associated with threat generalization (Bauer et al., 2020; Morriss et al., 2016; Nelson et al., 2015), and individuals with high intolerance of uncertainty are more likely to perceive ambiguous stimuli as threatening and engage in avoidance behavior to avoid the perceived threat (Hunt et al., 2019). Notably, these effects appear driven by stimuli in the middle of the CS+ to CS- generalization continuum, which are inherently the most ambiguous stimuli due to their perceptual equidistance to both threat and safety cues.

While intolerance of uncertainty and trait anxiety are highly correlated (Sexton and Dugas, 2009), intolerance of uncertainty may be particularly insightful in examining generalization, as the construct is theoretically well-aligned with the psychological and cognitive processes occurring while viewing generalized stimuli. No studies, to date, have examined how intolerance of uncertainty modulates neural responding during fear generalization. However, intolerance of uncertainty has been linked to aberrant responding in generalization relevant brain regions, including the amygdala, insula, and BNST (Grupe and Nitschke, 2013; Tanovic et al., 2018; Sarinopoulos et al., 2010; Shankman et al., 2014; Tanovic et al., 2018).

Current understanding of fear generalization in humans has been limited by shortcomings of neuroimaging technology. The spatial resolution of standard 3T field strength fMRI acquisition has constrained the ability to delineate the unique contributions of small neural regions or subdivisions implicated in generalization and threat responding. Although research suggests anxiety-related disorders are marked by behavioral and neural aberrancies related to fear generalization, a better understanding the precise neurobiological mechanisms involved in threat stimulus discrimination may ultimately help inform novel, targeted treatments.

In the current study, we aimed to utilize the high spatial resolution advantages afforded by 7T fMRI to characterize the neural circuits supporting threat discrimination and generalization. With this benefit, we specifically focused on a priori regions of interest (hippocampal subfields, amygdala subnuclei, BNST, habenula), using a novel experimental task based on prior fear generalization work. As a secondary aim, we set out to replicate prior work on some of the broader circuits supporting fear generalization by examining generalization effects within regions exhibiting functional discrimination between threat and safety during acquisition. Based on previous work on the neurobiology of conditioned fear generalization as well as threat processing more broadly - we hypothesized that activation of the CA1, amygdala (BLA, centromedial), BNST, habenula, insula, thalamus and caudate would generalize to the conditioned threat stimulus. We hypothesized activation of the dentate gyrus, CA3, precuneus, and vmPFC to generalize in an opposite pattern (i.e., to the CS-). Although we were not sufficiently powered to reliably detect effects related to individual differences, we conducted preliminary analyses to examine associations of neural activation to generalized threat stimuli with self-reported trait anxiety and intolerance of uncertainty to further probe the translational relevance of fear generalization; we hypothesized that these traits would be associated with greater generalization within regions such as the BNST, habenula, and CA1.

2. Material and methods

2.1. Participants

Forty-one undergraduate students were recruited from the University of Wisconsin – Milwaukee research subject pool. Eligible participants were between the ages of 18 and 55, right-handed, and English-speaking. Exclusion criteria included contraindications to MRI (e.g., irremovable metal in body, pregnancy, claustrophobia), use of specific medications (antipsychotics, anticonvulsants, mood stabilizers), and history of head trauma, neurological conditions, psychosis, or bipolar disorder. Participants were compensated with course credit and cash payment for their participation. Participants provided written informed consent. All study procedures were approved by the University of Wisconsin-Milwaukee and Medical College of Wisconsin Institutional Review Boards.

One participant was excluded due to technical error (no shocks administered during the task). Given a continuous reinforcement schedule during acquisition and healthy sample, nine subjects who failed a post-task contingency awareness test (simple selection between CS+ vs. CS-) were excluded from further analyses (though it may be advisable to use multiple outcomes to exclude non-learners; (Lonsdorf et al., 2019)). Included and excluded participants did not differ in any demographics or measures of interest. Sample characteristics are summarized in Table 1.

2.2. Procedure

2.2.1. Shock work-up

Prior to completing the fMRI generalization task, participants completed a shock work-up to determine the level of electrical stimulation (i.e., shock) used for the task at an individually-titrated aversive
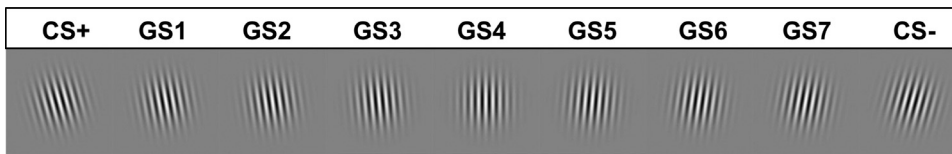
Fig. 1. Generalization stimuli (GS). From left to right, Gabor patch angle of orientation at $-15°$, $-10°$, $-8°$, $-5°$, $0°$, $+5°$, $+8°$, $+10°$, and $+15°$ offset from $0°$. The $-15°$ and $+15°$ degree stimuli were used as the CS+ and CS-, counterbalanced across participants.

Table 1

Sample characteristics ($n = 31$). STAI-T, State-Trait Anxiety Inventory – Trait; IUS, Intolerance of Uncertainty Scale.

	Mean (SD) / n (%)
Sex	
Female	20 (64.5%)
Male	11 (35.5%)
Age	22.61 (3.95)
Race/Ethnicity	
White, non-Hispanic	21 (67.7%)
Black/African-American	5 (16.1%)
Hispanic	3 (9.7%)
Asian/Pacific Islander	1 (3.2%)
Other/Unknown	1 (3.2%)
STAI-T	37.68 (8.55)
IUS	59.55 (16.21)

level. Shocks were delivered through a Psychlab system (Contact Precision Instruments, Cambridge, MA). Two electrodes were placed approximately two inches above the participant's left ankle. Starting at a low level of electrical stimulation ($\sim.6$ mA, duration=500 ms), a series of shocks were delivered. After each individual shock, participants were asked to make a 0 to 10 rating (0 = "didn't feel anything"t; 10 = "painful, but tolerable"). Participants were informed that the level set should be "painful, but tolerable" and would be used throughout the task ($M = 2.26$ mA, SD = 1.05 mA, range 0.98–4.9 mA).

2.2.2. Generalization task

The generalization task consisted of two phases: acquisition and generalization. During acquisition, participants were conditioned to the threat (CS+) and safety (CS-) cues. The acquisition phase consisted of a total of 20 trials (10 CS+, 10 CS-) in which the participant was presented with Gabor patches angled at either $+15°$ or $-15°$ offset from the vertical meridian ($0°$) (Fig. 1). The CS+ co-terminated with shock (100% reinforcement). Stimuli were counterbalanced such that for half of the participants, the $+15°$ Gabor patch was the CS+, while for the other half the $-15°$ stimulus was the CS+. Stimulus presentation was presented in a pseudorandomized order such that the same stimulus was presented a maximum of two consecutive trials. Stimuli appeared on the screen for 5000-ms. Participants viewed a fixation cross during inter-trial intervals (ITI) for 5000 to 9000-ms (average duration 7000-ms).

Immediately following acquisition, participants completed the generalization phase, in which 7 novel generalization stimuli (i.e., GSs) were introduced that varied in degree of similarity to the CS+ and CS-. GSs consisted of Gabor patches at $-10°$, $-8°$, $-5°$, $0°$, $+5°$, $+8°$, and $+10°$ offset from $0°$ (Fig. 1). The generalization phase consisted of 168 trials spread across three task runs. During each run, participants were presented with 6 trials of each GS and CS for 5000-ms. To prevent extinction, an additional 2 reinforced trials of the CS+ were included in each run. Thus, the generalization phase included a total of 18 trials of each GS and the CS- and 24 trials of the CS+ (25% reinforcement). Stimuli were presented in a randomized order. ITI duration varied from 2000 to 5000-ms (average duration 3500-ms).

Throughout both task phases, participants were instructed to make online behavioral ratings to evaluate perceived risk of the stimuli. For each trial, 1000-ms post-stimulus onset, participants were prompted with the text "Level of risk?" to make a 1–3 Likert rating (1 = "no risk"; 3 = "high risk") on a button box about the likelihood of being shocked

at the end of the trial. After responding, the number selected turned red on the screen; stimuli remained on the screen for the remainder of the 5000-ms stimulus presentation. The task design is depicted in Fig. 2. In addition, following the final generalization run, participants were presented with both the CS+ and CS- side-by-side on the screen and asked to indicate by button press which stimulus predicted the shock (nine subjects failed and were excluded from further analyses).

2.2.3. Trait anxiety

Trait anxiety was measured using the Trait version of the Spielberger State-Trait Anxiety Inventory (STAI-T; Spielberger, 1983). The STAI-T consists of 20 self-report items rated on a four-point scale and has demonstrated good psychometric properties, including high test-retest reliability (Barnes et al., 2002). Internal consistency in our sample was high (Cronbach's $\alpha = 0.914$).

2.2.4. Intolerance of uncertainty

Intolerance of uncertainty was measured using the Intolerance of Uncertainty Scale (IUS; Freeston et al., 1994; Buhr and Dugas, 2002). The IUS consists of 27 self-report items rated on a five-point scale. The IUS measures the extent to which an individual is able to tolerate uncertainty in ambiguous situations, beliefs about the emotional and behavioral consequences of uncertainty, and attempts to control the future. The IUS has demonstrated good internal consistency, test-retest reliability, and convergent/divergent validity with measures of anxiety, depression, and worry (Buhr and Dugas, 2002). Internal consistency was high in our sample (Cronbach's $\alpha = 0.929$).

2.3. MRI data acquisition

2.3.1. Anatomical

Imaging data were collected on a 7.0 Tesla MR950 General Electric scanner (GE Healthcare, Waukesha, WI). Whole-brain high-resolution T1-weighted anatomical images were acquired using a BRAVO gradient echo sequence with the following parameters: TR/TE = 8.012/3.784 s; FOV: 220 mm; flip angle = 5°; thickness = 0.8 mm; matrix = 276 × 276; voxel size = 0.43 × 0.43 × 0.80 mm. A high-resolution, T2-weighted structural scan covering the hippocampus was collected in order to create regions-of-interest (ROIs) based on parcellation of the hippocampal subregions. For the hippocampus anatomical scan, oblique images were acquired coronally, angulated perpendicular to the long axis of the hippocampal formation: TR/TE = 10,000 ms/30.66 ms; FOV: 85 mm; voxel size = 0.4297 × 0.4297 × 2 mm.

2.3.2. Functional

Partial-brain functional T2*-weighted EPI scans were acquired in an axial orientation with the following parameters: TR/TE = 2500 ms/24 ms; flip = 73°; FOV = 220 mm; matrix = 224 × 224; thickness = 1.8 mm; voxel size = 0.8594 × 08,594 × 1.8 mm. Partial-brain coverage was optimized to take advantage of the high-resolution capabilities of the 7T scanner and prioritize *a priori* ROIs of the study aims, including the amygdala, BNST, hippocampus, and insula. Scan coverage was determined on an individual subject basis by placing the most inferior slice to cover the most ventral part of the hippocampus and ensuring the most superior slice covered the superior insula (Fig. 3). An additional single-volume EPI scan with reverse phase encode polarity was collected after the task to correct for susceptibility-related distortion during image processing.
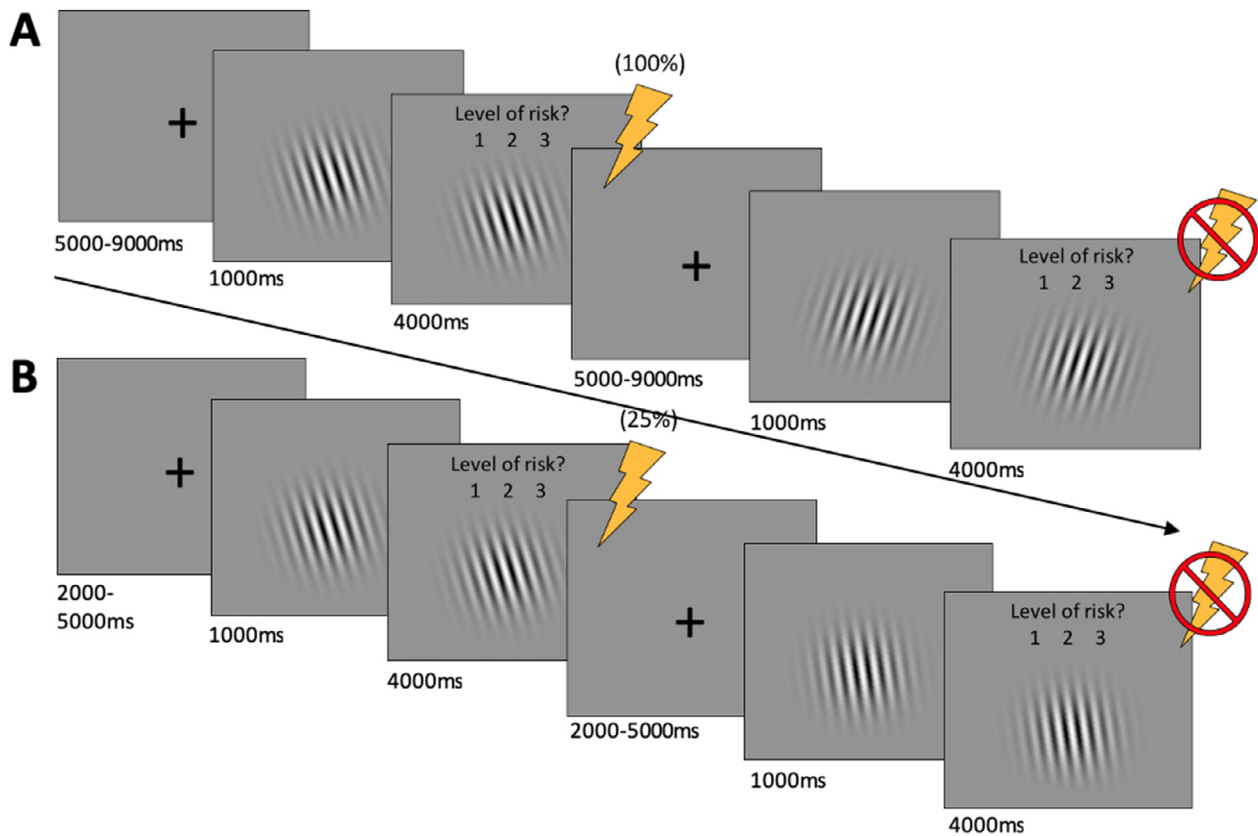
Fig. 2. Generalization task design. During acquisition (A), participants presented with 10 trials each of CS+ (co-terminated with shock on 100% of trials) and CS-. During generalization (B), participants presented with 18 trials each of the CS+ (unreinforced), CS-, and 7 generalization stimuli (GSs) that vary in orientation from the CSs. An additional 6 trials of the reinforced CS+ were presented to prevent extinction. Two trials are depicted for each phase (A: CS+ and CS- trials; B: CS+ and GS1 trials).
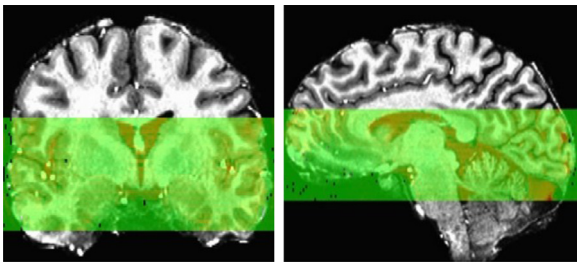

Fig. 3. Example EPI partial coverage from a representative subject.

2.4. Preprocessing

Data were analyzed using Analysis of Functional Neural Images (AFNI) software (Cox, 1996). In preprocessing, the first three volumes were removed to allow for scanner equilibration, and volumes with excessive motion (>0.2 mm frame-to-frame Euclidean norm derivative) and/or outliers (>10% of voxels in the volume identified as outliers) were excluded from further analyses. Due to greater sensitivity to distortion at ultra-high field, remaining EPI volumes were distortion corrected by warping to a middle space with the reverse phase encode polarity scan. EPI volumes were co-registered to the first functional volume, aligned to the subject's anatomy, and converted to percent signal change. A blur of 2 mm FWHM was applied to the data. For whole brain group analyses, data were normalized to template (MNI152). Single subject BOLD responses were modeled with regressors for each condition

type (acquisition: CS+, CS-; generalization: CS+, GS1, GS2, GS3, GS4, CS-) for each voxel in the functional dataset. To eliminate confounding effects of electric shock on BOLD signal and ensure an equal number of stimulus presentations per condition, parameter estimates for reinforced CS+s were modelled separately and excluded from further analysis. Motion parameters were included as regressors of no interest. As the study's primary aim was to examine generalization of threat, analysis of GSs focused on stimuli (GS1–3) expected to generalize to the threat stimulus based on their angle of orientation, along with GS4 (i.e., the vertical stimulus which was dissimilar from both the CS+ and CS-). To explore neural processing of safety cues, analyses were repeated modelling the stimuli expected to generalize to the CS- (i.e., CS-, GS7, GS6, GS5, GS4, CS+); these results are reported in Supplemental Material.

2.5. ROI definition

2.5.1. Functional ROIs

The acquisition run was used to define functional ROIs sensitive to differential conditioning (e.g., (Lissek et al., 2014a)). Data were preprocessed as described above; however, a 4 mm – rather than 2 mm – smoothing kernel was used to blur the data in order to produce larger, contiguous clusters for better interpretability. Voxelwise analyses of the CS+ vs. CS- contrast were conducted using a voxelwise probability of $p < 0.001$ and cluster probability of $p < .05$. Estimated blur of the final EPI dataset was calculated using 3dFWHMx. Average auto-correlation function (ACF) parameters were entered into 3dClustSim to correct for multiple comparisons and estimate probability of obtaining clusters of a particular size ($p < .05$, $k > 217$).
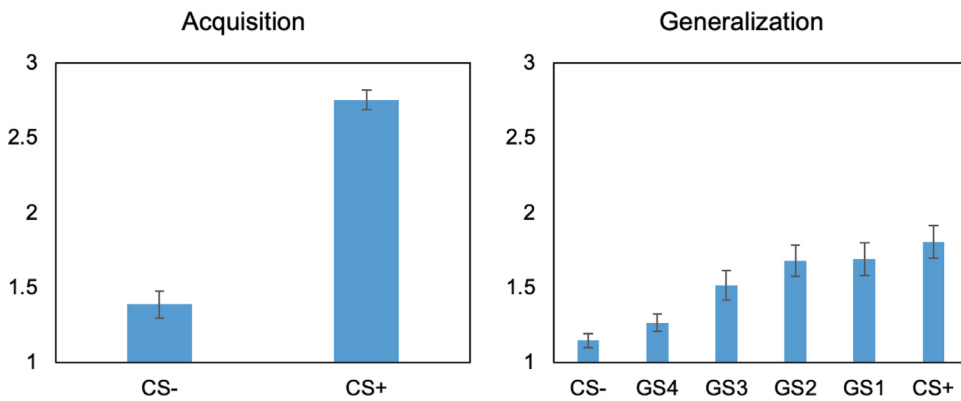
2.5.2. Anatomical ROIs

Subjects' native space T1 and T2 weighted structural scans were entered into Automatic Segmentation of Hippocampal Subfields (ASHS) software for hippocampal parcellation. Segmentation was performed using the Magdeburg 7T young adult protocol (Berron et al., 2017). ASHS has been validated in 7T data where it has demonstrated comparable accuracy with manual segmentation (Giuliano et al., 2017). The segmentation protocol failed for one participant, who was subsequently excluded from hippocampal analyses.

Freesurfer version 6.0 was used for automated segmentation of amygdala subnuclei (basal, lateral, and centromedial) from subjects' native space T1 anatomical volume (Saygin et al., 2017).

The BNST ROI was defined in MNI space by the probabilistic segmentation mask constructed by Theiss and colleagues (Theiss et al., 2017).

Based on average coordinates from a meta-analysis of the human habenula (Lawson et al., 2013), spherical ROIs with a radius of 2 mm were created in MNI space for the left (−2.8, −24.4, 2.3) and right (4.8, −24.1, 2.2) habenula. The left and right habenula ROIs were combined for a bilateral habenula mask.

2.6. Data analysis

2.6.1. BOLD activation

Beta weights during the generalization phase were averaged across voxels within the functional and *a priori* ROIs and plotted across the conditioned (i.e., CS+, CS-) and generalization stimuli. A series of one-way ANOVAs with six levels (CS+, GS1, GS2, GS3, GS4, CS-) were conducted to examine generalization effects on threat stimulus processing and were followed by tests of linear and quadratic components, as appropriate. Statistical threshold was set at $\alpha = 0.05$, using the Benjamini-Hochberg procedure to correct for multiple comparisons.

2.6.2. Associations with individual differences in anxiety

Consistent with prior work in human fear generalization research (see (van Meurs et al., 2014; Kaczkurkin et al., 2017; Lange et al., 2019)), linear departure scores (LDS) were calculated to correlate with individual difference factors (i.e., STAI-T and IUS). The LDS assesses the degree to which an individual subject's generalization gradient deviates from linearity and is typically derived from the following equation: LDS = (GS1 + GS2 + GS3)/3 – (CS+ - GS4)/2. In this equation, the second term refers to the theoretical midpoint if the gradient were perfectly linear, while the first expression represents the average response to the three generalized threat stimuli, which may fall above (positive departure), below (negative departure), or at (zero departure) the theoretical linear midpoint. In the current study, the GS4 (i.e., the vertical GS) was used in place of the CS-, as it represents a distinct, dissimilar stimulus from the CS+, and we did not expect a linear relationship to extend across the entire dimension of threat (GS1–3) and safety (GS5–7) generalization stimuli. The LDS represents a single, quantifiable index

of generalization. Positive LDS values represent shallow, convex gradients, while negative LDS values represent steep, concave gradients, with positive and negative departures indicating stronger and weaker generalization, respectively. For each functional and a priori ROI, extracted averaged beta weights were used to generate an LDS for that ROI and were correlated with STAI-T and IUS scores. Given the shared variance of STAI-T and IUS, we also entered both scores into a series of multiple regressions predicting each ROI's LDS to examine potential unique contributions of these traits. Finally, due to our modified equation, we also conducted a series of paired t-tests to examine whether BOLD response varied between the CS- and GS4 for each ROI. These tests were significant for the habenula and BNST, which were excluded from correlational LDS analyses, as this suggested the GS4 was an inappropriate replacement for the CS-.

2.6.3. Behavioral data

Levels of conditioning during acquisition and generalization were assessed with paired samples t-tests to compare risk ratings to the CS+ vs. CS-. Risk ratings during generalization were analyzed with a one-way, repeated measures ANOVA with six levels (CS+, GS1, GS2, GS3, GS4, and CS-) and followed by tests of linear and quadratic components. An LDS was also calculated for perceived risk ratings during the generalization task and correlated with STAI-T and IUS scores. Statistical threshold was set at $\alpha = 0.05$ for all tests.

3. Results

3.1. Behavioral

3.1.1. Acquisition

Behavioral results are presented in Fig. 4. Paired samples t-tests demonstrated significantly higher perceived risk for the CS+ ($M = 2.75$, SD=0.37) compared to the CS- ($M = 1.34$, SD=0.49) during conditioning, $t(30)=10.74$, $p<.001$. There were no significant differences in reaction time between the conditioned stimuli ($p=.36$). STAI-T trait anxiety was significantly correlated with higher perceived risk of the CS- ($r = 0.474$, $p=.007$). IUS was not significantly correlated with CS- ratings ($r = 0.332$, $p=.07$). There were no significant correlations between STAI-T or IUS with CS+ ratings or reaction times for either stimulus.

3.1.2. Generalization

Conditioned fear was maintained during the generalization runs, as evidenced by significantly higher perceived risk for the CS+ ($M = 1.80$, SD=0.61) compared to the CS- ($M = 1.15$, SD=0.25), $t(30)=5.55$, $p<.001$. A repeated measures ANOVA revealed significantly increased risk ratings from the CS- to GS4 to GS3 to GS2 to GS1 to CS+, $F(5,26)=22.49$, $p<.001$, indicating generalization of conditioned fear. Follow-up comparisons indicated both linear, $F(1,30)=31.52$, $p<.001$, and quadratic, F(1,30)=4.78, $p=.03$, components to the generalization gradient. Additional follow-up tests of repeated contrasts showed

Table 2

Significant clusters for contrast CS+ > CS- during acquisition phase with voxel-wise threshold $p < .001$ and cluster size corrected threshold of $p < .05$, $k > 217$.

	Region	k	Volume (mm³)	MNI coordinates			
				x	y	z	t
1	Visual cortex/lingual gyrus	2142	2847	0	−77	−4	4.91
2	Visual cortex/lingual gyrus	1211	1609	−16	−102	1	4.72
3	R insula	1120	1488	45	−7	11	5.64
4	Cuneus	877	1166	25	−96	31	4.82
5	L insula	490	651	−34	−15	−4	4.12
6	R inferior parietal lobule/somatosensory cortex	489	650	51	−30	18	4.57
7	Somatosensory cortex/posterior insula	423	562	−51	−7	13	5.07
8	L inferior parietal lobule/somatosensory cortex	331	440	−47	−35	28	4.33
9	Somatosensory cortex	327	435	60	−3	14	4.60
10	Fusiform gyrus	284	377	25	−63	−10	4.60
11	Cuneus	245	326	17	−82	26	4.69
12	R thalamus	236	314	13	−26	17	4.48
13	L thalamus	218	290	−4	−16	2	5.13

ratings differed between all adjacent stimuli, with the exception of GS1-GS2. There was also a significant effect of condition on reaction time, $F(5,26)=2.96$, $p=.01$, with a significant quadratic component, $F(1,30)=4.95$, $p=.03$, indicating increased reaction time for generalization stimuli in the middle of the generalization continuum (e.g., GS2, GS3).

3.2. fROI definition

Using a voxel-wise $p<.001$ and cluster threshold of $p<.05$, 13 clusters emerged that demonstrated increased activation for the CS+ relative to the CS- during acquisition (Table 2). No clusters emerged that demonstrated increased activation for the CS- relative to the CS+.

3.3. Generalization effects

3.3.1. fROIs

Full results of the within-subjects generalization tests for all fROIs identified during the acquisition phase and a priori ROIs are presented in Table 3. During the generalization phase, activation within several fROIs demonstrated positive generalization gradients, with strongest activation to the CS+ with gradually decreasing activation to the GS1, GS2, GS3, GS4, and CS- as stimuli were increasingly dissimilar to the CS+ (see Fig. 5). Specifically this pattern was noted in both of the visual cortex fROIs (cluster 1: $F(3.382, 26) = 3.516$, $p = .042$; cluster 2: $F(3.397, 26) = 2.97$, $p = 0.045$) and thalamus fROIs (cluster 12: $F(3.796, 26) = 4.7$, $p = .008$; cluster 13: $F(5,26) = 3.855$, $p = .006$). Follow-up tests of linear and quadratic components of these effects indicated significant linear, but not quadratic, effects in the more posterior visual cortex cluster (2), $F(1,30) = 6.139$, $p = .019$, right thalamus, $F(1,30) = 16.134$, $p < .001$, and left thalamus, $F(1,30) = 15.817$, $p < .001$. For the other cluster in the visual cortex (1), both linear, $F(1,30) = 7.054$, $p = .013$, and quadratic, $F(1,30) = 5.039$, $p = .032$, components were significant.

3.3.2. Hippocampal subfields

Negative generalization gradients, with strongest activation to the CS- with gradually decreasing activation to the GS4, GS3, GS2, GS1, and CS+ as stimuli were increasingly similar to the CS+, were observed in the dentate gyrus, $F(5,25) = 2.919$, $p = .045$, CA3, $F(5,25) = 2.778$, $p = .03$, and CA1, $F(5,25) = 2.46$, $p = .036$ (Fig. 6). Follow-up tests indicated significant linear, but not quadratic effects in these regions (dentate gyrus: $F(1,29) = 8.868$, $p = .006$; CA3: $F(1,29) = 6.422$, $p = .017$; CA1: $F(1,29) = 11.756$, $p = .002$).

3.3.3. Amygdala subnuclei

There was a marginally significant negative generalization gradient observed in the basal nucleus of the amygdala, $F(3.809, 25) = 2.301$,

Table 3

Results of repeated measures ANOVAs for functional (fROIs) and a priori regions of interest. Results are clustered by region with fROI cluster numbers in parentheses corresponding to those denoted in Table 2. Benjamini-Hochberg procedure was used to correct for multiple comparisons; adjusted p-values are reported in the table.

ROI	F	p
fROIs		
Visual cortex/lingual gyrus (1)	3.516	0.042
Visual cortex/lingual gyrus (2)	2.97	0.045
Cuneus (4)	0.686	0.566
Cuneus (11)	1.4	0.454
Fusiform gyrus (10)	1.189	0.319
R insula (3)	0.525	0.999
L insula (5)	0.367	0.871
R inferior parietal lobule/somatosensory cortex (6)	0.345	0.754
L inferior parietal lobule/somatosensory cortex (8)	1.333	0.999
Somatosensory cortex/posterior insula (7)	0.903	0.641
Somatosensory cortex (9)	1.229	0.606
R thalamus (12)	4.7	0.008
L thalamus (13)	3.855	0.006
Hippocampal subfields		
Dentate gyrus	2.919	0.045
CA1	2.46	0.036
CA3	2.778	0.03
Amygdala, BNST, & Habenula		
Basal amygdala	2.301	0.09
Lateral amygdala	1.329	0.191
Centromedial nucleus	1.511	0.19
BNST	2.963	0.042
Habenula	3.926	0.002

$p = .09$, with a significant linear, but not quadratic, component, $F(1,29) = 8.94$, $p = .006$ (Fig. 7). There were no significant generalization effects observed in the lateral or centromedial subnuclei.

3.3.4. BNST

Significant generalization was observed in the BNST, $F(5,26) = 2.963$, $p = .042$; however, follow-up tests revealed that activation within the BNST was neither linear ($p = .082$) nor quadratic ($p = .208$) in nature (Fig. 8). Results of a paired t-test indicated BNST BOLD response to the GS4 was significantly greater than that of the CS-. We conducted an additional ANOVA with all nine stimuli (i.e., CS+, CS-, GS1–7), which did not reach significance, $F(8,23) = 1.933$, $p = .056$, though follow-up tests suggested there was a cubic pattern to this gradient.
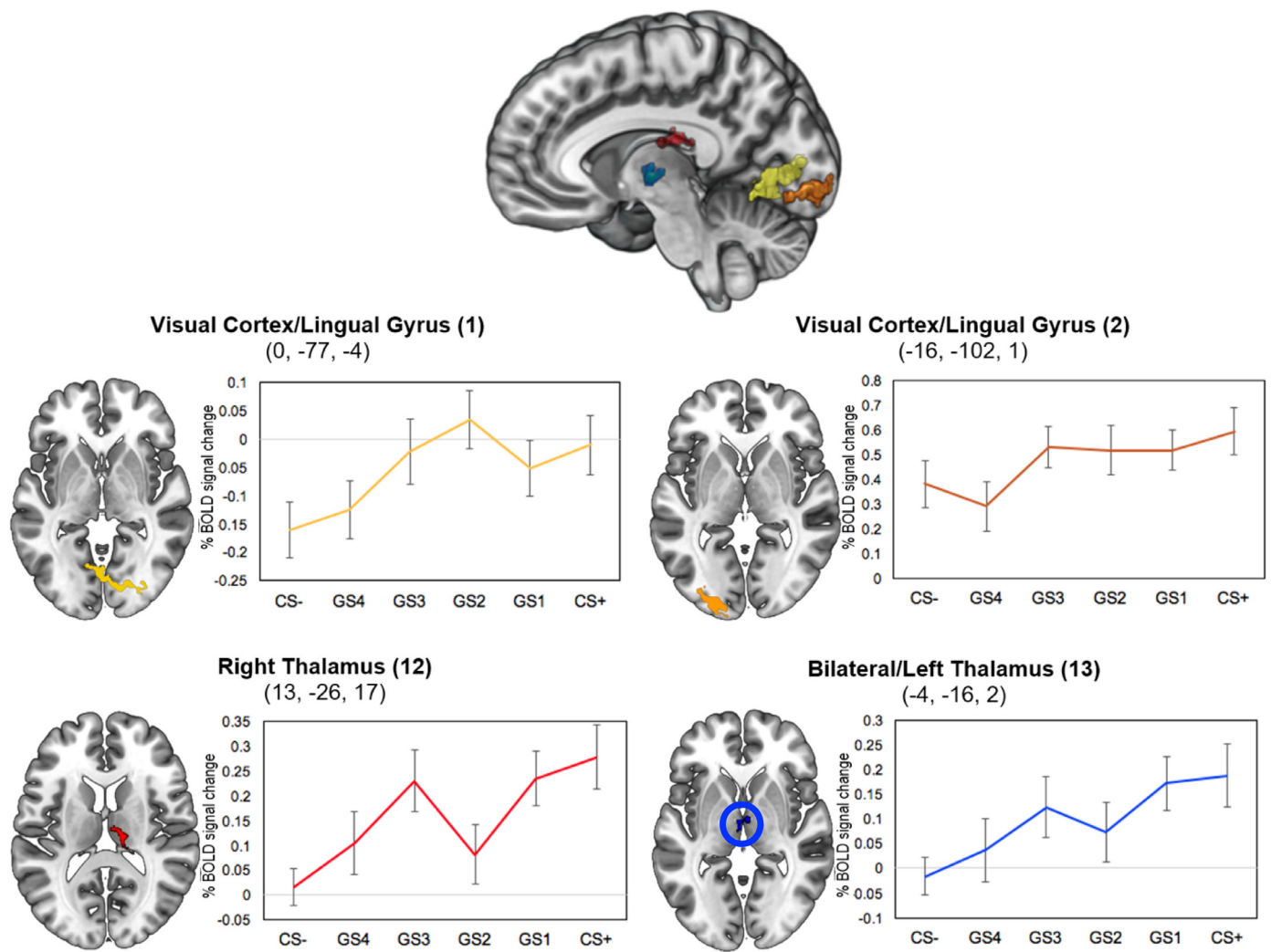
Fig. 5. Functional regions-of-interest (fROIs) demonstrating significant effects during threat generalization. Numbers in parentheses correspond to the cluster numbers presented in Table 2. Parameter estimates represent signal averaged across the fROIs for the conditioned threat (CS+) and safety (CS-) cues, along with generalization stimuli (GSs). Error bars represent standard error of the mean.
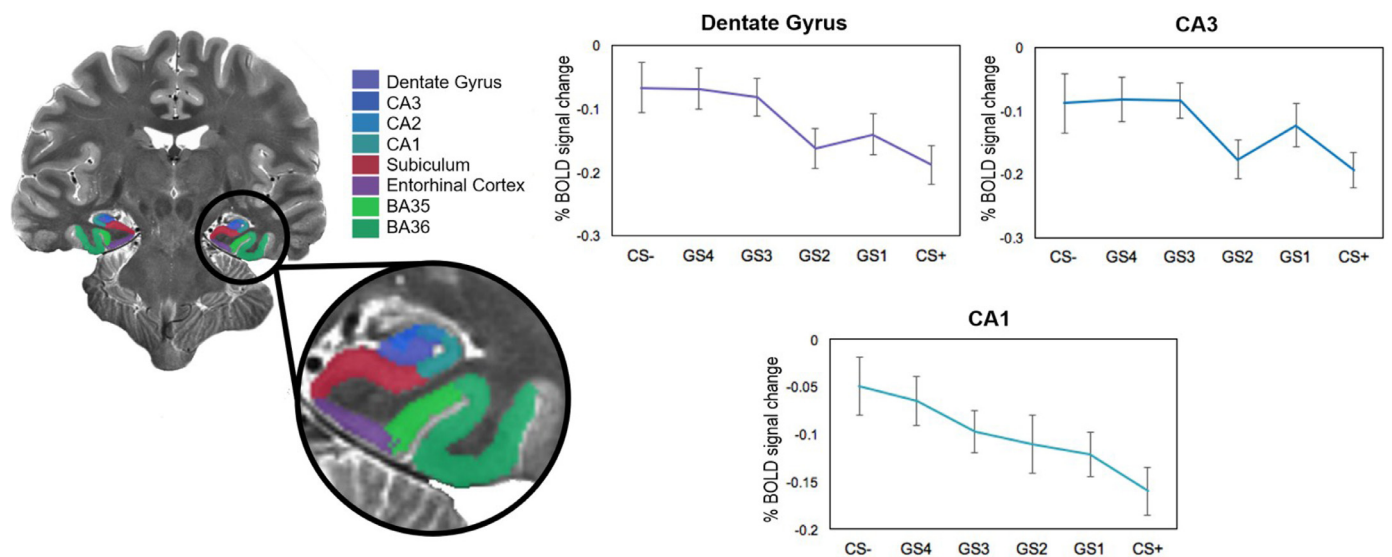

Fig. 6. Hippocampal segmentation of a representative subject presented on T2-weighted anatomical scan. In line with a priori hypotheses, effects of fear generalization were examined in the dentate gyrus, CA3, and CA1 subfields. Significant negative generalization effects were observed in all three regions. Parameter estimates represent signal averaged across the hippocampal subfields for the conditioned threat (CS+) and safety (CS-) cues, along with generalization stimuli (GSs). Error bars represent standard error of the mean.
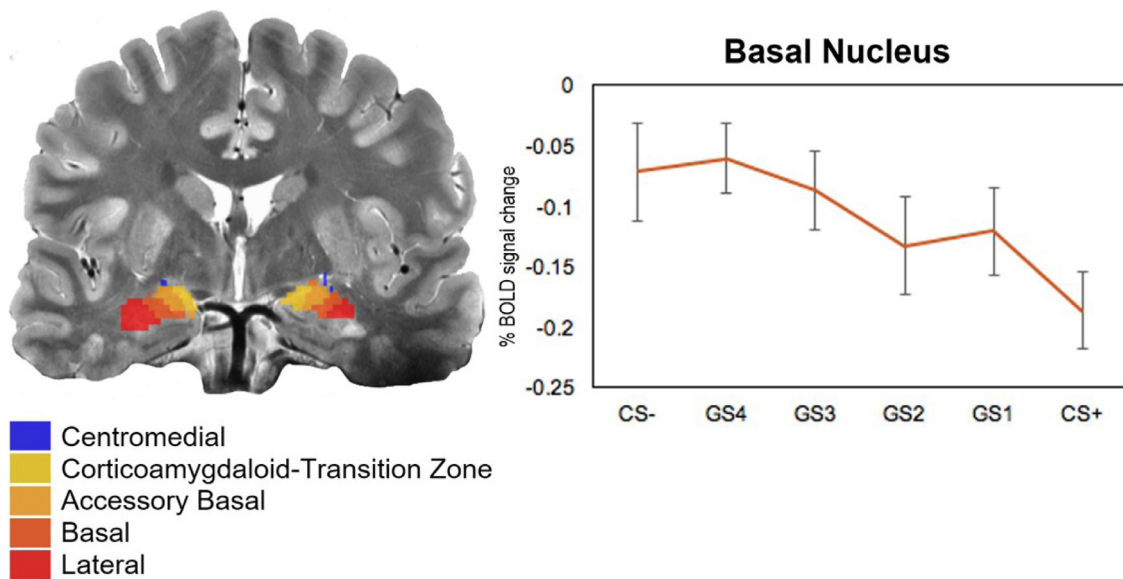
Fig. 7. Segmentation of amygdala subnuclei for a representative subject presented on T2-weighted anatomical scan. Marginally significant ($p = .09$) negative generalization effects were observed in the basal nucleus. Parameter estimates represent signal averaged across the hippocampal subfields for the conditioned threat (CS+) and safety (CS-) cues, along with generalization stimuli (GSs). Error bars represent standard error of the mean.
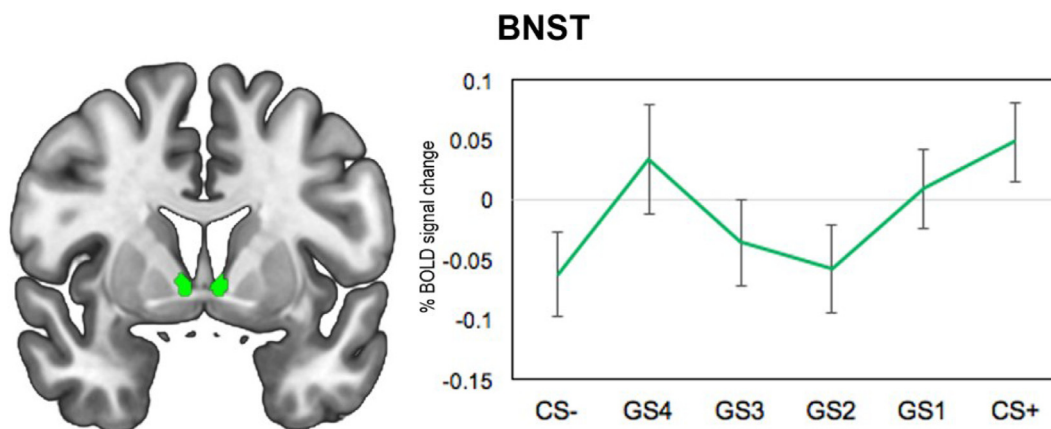

Fig. 8. Bed nucleus of the stria terminalis (BNST) ROI defined in MNI space using probabilistic segmentation mask (Theiss et al., 2017) . Parameter estimates represent signal averaged across the BNST for the conditioned threat (CS+) and safety (CS-) cues, along with generalization stimuli (GSs). Error bars represent standard error of the mean.

3.3.5. Habenula

A significant positive generalization gradient was observed in the habenula, $F(5,26) = 3.926$, $p = 0.002$, with a significant linear component to this effect, $F(1,30) = 8.465$, $p = .007$ (Fig. 9). The quadratic component was marginally significant, $F(1,30) = 3.109$, $p = .088$. Habenular response significantly varied between most adjacent stimuli. For this reason, we conducted an additional omnibus test including all nine stimuli (Supp. Fig 2). There was a significant positive generalization gradient across the entire CS- to CS+ spectrum, $F(8,23) = 3.40$, $p = .001$, with a significant linear, $F(1,30) = 13.02$, $p = .001$, but not quadratic component.

3.4. Associations with individual differences

Significant associations of linear departure scores (i.e., difference between GS1–3 and theoretical linear midpoint between CS+ and GS4) with individual differences are presented in Fig. 10. Higher STAI-T trait anxiety was positively correlated with linear departure scores (i.e., greater generalization) in the primary somatosensory cortex, $r = 0.39$,

$p = .03$ (cluster 9). STAI-T scores were not correlated with any other ROIs.

Total IUS was positively correlated with linear departure scores in the right insula (cluster 3; $r = 0.379$, $p = .036$) and primary somatosensory cortex (cluster 9; $r = 0.373$, $p = .039$). IUS scores were not correlated with any other ROIs.

Results of multiple regression models including both STAI-T and IUS as explanatory variables did not indicate any significant effects (all p's > 0.089).

4. Discussion

In a sample of healthy young adults, the current study sought to characterize the neural processes contributing to the generalization of conditioned fear using a novel experimental task. Supporting prior work, BOLD signal tracked along gradients for a conditioned threat stimulus and perceptually similar stimuli in several key brain regions (e.g., thalamus, hippocampus). Moreover, the novel use of high-resolution 7T fMRI provided improved spatial resolution that highlighted the importance of
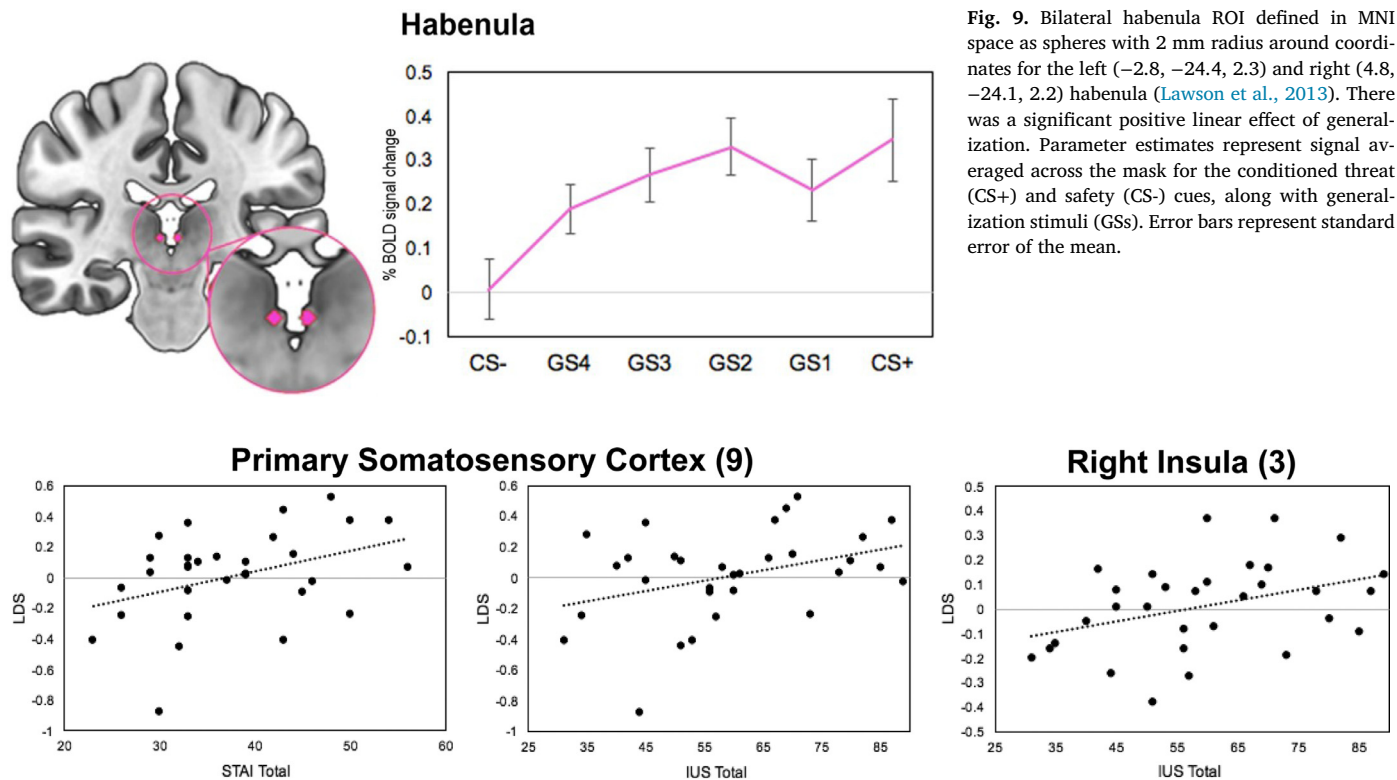
Habenula

Fig. 9. Bilateral habenula ROI defined in MNI space as spheres with 2 mm radius around coordinates for the left (−2.8, −24.4, 2.3) and right (4.8, −24.1, 2.2) habenula (Lawson et al., 2013). There was a significant positive linear effect of generalization. Parameter estimates represent signal averaged across the mask for the conditioned threat (CS+) and safety (CS-) cues, along with generalization stimuli (GSs). Error bars represent standard error of the mean.

Fig. 10. Scatterplots depict significant associations of self-reported trait anxiety (STAI) and intolerance of uncertainty (IUS) with linear departure scores (LDS) for regions-of-interest. The LDS was calculated by extracting averaged beta weights for each ROI and condition and entering them in the formula: LDS = (GS1+GS2+GS3)/3 − (CS+ - GS4)/2. Positive and negative LDS values represent stronger and weaker generalization, respectively. STAI and IUS scores were positively correlated with generalization in the primary somatosensory cortex (60, −3, 14; cluster 9). IUS was also positively correlated with generalization in the right insula (45, −7, 11; cluster 3).

previously uninvestigated small neural regions (e.g., habenula) during threat stimulus generalization.

Analysis of the initial conditioning run revealed a diffuse network of regions – including the insula, inferior parietal lobule, and somatosensory cortices - that exhibited greater activation for the threat versus safety cue; however, when novel generalization stimuli were introduced, only regions within the visual cortex and thalamus exhibited significant generalization, with the BOLD response tracking along the continuum of similarity to the CS+. While many emphasize the amygdala's role in threat detection and arousal (Davis, 1992; LeDoux, 2003), sensory input must first be transmitted to the amygdala along thalamic mediated paths (Das et al., 2005; Shi and Davis, 2001). As such, early perceptual processing plays an important role in fear generalization (Struyf et al., 2015). Psychophysiological studies have demonstrated enhanced visuocortical activation for stimuli associated with threat (Armony and Dolan, 2001; Miskovic and Keil, 2012, 2013; Vuilleumier and Driver, 2007). The current findings suggest a possible tuning effect, where this enhanced visual processing is perhaps weighted depending on degree of similarity to the learned threat cue (McTeague et al., 2015; Stegmann et al., 2020). This pathway may have important clinical relevance, as prior work has shown anxiety modulates early, low-level visual processing (Ferneyhough et al., 2013).

Notably, in the current study, we also found a marginally significant effect of generalization in the basal nucleus of the amygdala. The basolateral nucleus receives visual input from higher-order visual association cortices (Pessoa and Adolphs, 2010; Shi and Davis, 2001) and is thought to be a convergence zone for affective modulation of sensory information (Shi and Davis, 2001). Feedback loops between the lateral and basal nuclei of the amygdala may also modulate visual processing (Freese and Amaral, 2005; Pessoa and Adolphs, 2010). Interestingly, in contrast to our hypothesis, the effect of generalization in the basal amygdala was

negative, such that there was *less* activation as stimuli were increasingly similar to the CS+. Previous work has found similar negative generalization gradients in the amygdala/hippocampus (Kaczkurkin et al., 2017). Together with the generalization findings in the earlier parts of the processing stream (i.e., visual cortex, thalamus), it is possible that the amygdala is less critical for further processing as the response has already been modulated by more basic sensory regions. Despite its prevalence in models of fear and anxiety (Davis, 1992; Etkin and Wager, 2007), the amygdala is surprisingly inconsistent in fear conditioning research, with meta-analytic work failing to characterize robust amygdala response to conditioned threat versus safety cues (see Fullana et al., 2016). We also did not observe greater amygdala response to the CS+ over CS- during acquisition in the current study. Moreover, neuroimaging studies have also mostly failed to reveal generalization gradients within the amygdala (Greenberg et al., 2013; Lange et al., 2019), though altered functional connectivity of the amygdala (including with visual areas) may be important (Morey et al., 2015; Dunsmoor et al., 2011; Lissek et al., 2014a).

The current findings also underscore the importance of the hippocampus in fear generalization, as we found strong evidence of its sensitivity to generalization, even within a task that varied somewhat from previous work. The hippocampus has been proposed as the heart of neural models of fear generalization (Lissek et al., 2014a). Specifically, sensory information is relayed via the thalamus and higher order visual cortices to the hippocampus, where – depending on the degree of perceptual overlap between a novel, ambiguous stimulus and learned threat cue – a pattern completion or separation process occurs to elicit or inhibit fear. Consistent with hypotheses, the dentate gyrus and CA3 (implicated in pattern separation; Clelland et al., 2009; McHugh et al., 2007; Rolls, 2013; Yassa and Stark, 2011) both demonstrated significant negative generalization effects, such that there was increased activation

within these subfields as stimuli were increasingly *dis*similar from the CS+, suggesting pattern separation was occurring. In the context of fear generalization, these findings suggest that the dentate gyrus and CA3 play an active role in discriminating between stimuli that are perceptually similar to a learned threat cue.

On the other hand, contrary to hypotheses, a similar negative effect was also observed in the CA1. Functional studies of the hippocampal subfields in humans are limited, though evidence has suggested that the CA1 is biased towards pattern completion (Bakker et al., 2008; Lacy et al., 2011; Dimsdale-Zucker et al., 2018). Although in the current study, functional connectivity of the dentate gyrus and CA1 did not significantly vary as an effect of condition (see Supplemental), examination of individual contrasts hints that the CA1 is perhaps coactivated with fear excitatory regions (e.g., amygdala, thalamus) for stimuli similar to threat. These effects were small and did not survive corrections but do fit with the theory that the CA1's pattern completion process facilitates engagement of fear excitatory structures to produce anxious arousal. That said, it is unclear why the activation of the CA1 was less robust as stimuli were more similar to the CS+.

Rodent models propose a complex picture of hippocampal subfield function, suggesting that the CA3 may facilitate both pattern completion and separation depending on the degree of overlap between a novel stimulus and its existing neural schema (Guzowski et al., 2004). As the CA3 outputs to the CA1, the consequences of dynamic competition within the CA3 may have additional downstream effects on computations within the CA1 that may (or may not) lead to pattern completion. Recent evidence has also shown that lesions of the CA1 impair pattern separation in humans (Hanert et al., 2019). Thus, the CA1 may also have a dynamic function and support both matching *and* discrimination, and this role may be influenced by the input it receives from the CA3. Few neuroimaging studies, though, have examined pattern separation and completion in humans with sufficient spatial resolution to reliably distinguish between subfields. In addition, studying fear generalization is quite complex given an inherent association of pattern separation with memory processes of encoding and recall in such paradigms (Aimone et al., 2011; Hunsaker and Kesner, 2013). Suggesting that the CA1 is primed for pattern completion may, therefore, be an overly simplistic representation of its function. Future work would benefit from probing the unique and shared functions within and between human hippocampal subfields and downstream structures. A clearer model of these mechanisms is essential for understanding how processes may go awry in pathological anxiety.

Significant generalization of the conditioned threat stimulus was also observed in the bilateral habenula. In fact, habenula response significantly decreased across the entire continuum of generalization stimuli between the CS+ and CS-. The habenula is thought to play an important role in signaling the occurrence of salient negative events in order to modulate behavior adaptively (Boulos et al., 2017; Epstein et al., 2018; Salas et al., 2010). While prior research in humans has demonstrated activation of the habenula in response to conditioned threat cues (Hennigan et al., 2015; Lawson et al., 2017), this study is the first to show that this activation generalizes to perceptually-similar cues in a linear fashion. While it would be valuable for future work to examine habenular activation within previously validated generalization paradigms, the current findings suggest that, as stimuli become more similar to a learned threat, habenular response increases. Given that the habenula is thought to modulate experience-dependent emotional behavior (Boulos et al., 2017; Epstein et al., 2018; Salas et al., 2010), this may influence approach-avoidance behaviors to perceived threats. This has important clinical relevance, as avoidance is a key behavioral feature of anxiety-related disorders.

Abnormal activation of the habenula may perhaps reflect errors in threat prediction that subsequently contribute to maladaptive behavioral and emotional response (e.g., avoidance, fear). The habenula is part of a complex, diffuse network that includes prefrontal (Ely et al., 2016; Shelton et al., 2012; Torrisi et al., 2017) and brain-

stem (Boulos et al., 2017; Epstein et al., 2018) regions that may give rise to these responses. Although in the current study we did not observe modulation of the habenula based on individual differences in anxious traits, future studies would benefit from consideration of the habenula in psychopathology to better understand its role.

Clarifying the effects of anxiety on BNST activity may also be critical. In the current study, although there was a main effect of stimulus, it was difficult to interpret the meaning of this effect given that it was neither linear nor quadratic in nature. The BNST is thought to be particularly related to sustained threat-related arousal, i.e., anxiety (Davis et al., 2010; Klumpers et al., 2017). This conceptualization, however, has become scientifically contentious, as emerging evidence has suggested the BNST cannot be functionally differentiated from the amygdala (Hur et al., 2020; Shackman and Fox, 2016). That said, our results do fall in line with theory proposing they support different facets of threat responding. Specifically, we observed greater activation in the BNST for stimuli most similar to the CS+, suggestive of apprehension about the threat cue; though we hypothesized this same effect for both the BNST and basolateral nucleus of the amygdala, our analysis revealed effects in opposite directions. For the BNST, there was also robust activation for the GS4. Given that the vertical orientation of the GS4 was dissimilar from both the conditioned threat and safety cues, it may have been perceived as more ambiguous; therefore, increased BNST activation for this stimulus may be consistent with increased anxious apprehension during uncertain threat (Alvarez et al., 2011). Further work should aim to clarify how the BNST and amygdala may or may not be functionally differentiated, especially in the context of fear generalization.

Surprisingly, the effects of individual differences in anxious traits on fear generalization within the brain were sparse. Overgeneralization of fear has been observed across a number of anxiety-related disorders (Ahrens et al., 2016; Cha et al., 2014; Lissek et al., 2009, 2014b; Stegmann et al., 2020; Thome et al., 2018). Moreover, emerging research has suggested that this overgeneralization is also reflected in the brain regions supporting this process (Cha et al., 2014; Greenberg et al., 2013; Kaczkurkin et al., 2017; Morey et al., 2020). In the current study, trait anxiety was related only to greater generalization (as defined by LDS) in the primary somatosensory cortex, while intolerance of uncertainty was related to greater generalization within the right insula and primary somatosensory cortex. These findings, though preliminary and within a novel task paradigm, are consistent with prior work in clinical populations (Cha et al., 2014; Kaczkurkin et al., 2017; Morey et al., 2020).

Given the study's sample size, it is most likely that we were underpowered to reliably detect true associations between anxiety and BOLD response; in this context, it is possible these reported findings may not replicate. Power issues also likely explain the sparsity of our findings, though it is possible several factors may have limited the influence of individual differences. For instance, despite sufficient variability in self-reported anxiety, this was, overall, a relatively healthy sample. Overgeneralization may be more robust in samples with clinical anxiety (Stegmann et al., 2019). Indeed, studies examining whether subclinical trait anxiety is associated with overgeneralization are mixed (Haddad et al., 2013; Wong and Lovibond, 2018; Arnaudova et al., 2017; Torrents-Rodas et al., 2013). A recent meta-analysis supports a small positive effect of anxious traits on generalization (Sep et al., 2019). It is notable, however, that many inconsistencies in moderating effects of anxious traits on fear conditioning and generalization may be due to wide variability in methodology and unreported and underpowered analyses (Lonsdorf and Merz, 2017). It is imperative that future work implements rigorous and transparent methods in larger samples to shed light on true findings and avoid contributing to irreplicable, misleading results.

Additionally, although a useful metric that has validated clinical correlates (Lange et al., 2019; van Meurs et al., 2014), the linear departure score is also a somewhat crude measure that may not adequately characterize potentially meaningful intraindividual patterns of respond-

ing (e.g., poor differentiation between conditioned threat and safety cues). Recent work has utilized data-driven clusterizing approaches to characterize individual patterns of behavioral fear generalization (Stegmann et al., 2019). Diverging from classic perspectives on fear generalization (which typically distinguish between linear and quadratic gradients), this study found five distinct response patterns characterizing generalization; importantly, a pattern defined by a linear gradient with high arousal and low CS-differentiation had the highest levels of self-reported anxiety. In our sample, trait anxiety was highly correlated with greater perceived risk of the CS-, consistent with the notion that pathologic anxiety may be characterized by elevated fear responding to safety cues (Duits et al., 2015; Gazendam et al., 2013). Utilizing data-driven approaches to define more nuanced patterns of responding during generalization may also be important for understanding how anxious traits relate to behavioral and neural fear generalization and identify whether a distinct "at risk" group exists.

Although we employed a novel generalization task, taken together, our findings were largely consistent with extant literature, with regions like the hippocampus and thalamus appearing to play an important role in this process; moreover, we found that several previously unexplored regions (such as the habenula) support fear generalization. That said, the current findings diverge from prior work in several notable ways. The functionally-derived ROIs in the current study were similar to those identified in other fear generalization and conditioning neuroimaging studies (Dunsmoor et al., 2011; Lissek et al., 2014a). These studies, however, have found that many more regions were sensitive to effects of generalization, whereas our findings observed generalization effects only within the visual cortex and thalamus. In particular, the insula is especially sensitive to uncertainty (Grupe and Nitschke, 2013; Simmons et al., 2008; Singer et al., 2009) and has been consistently implicated in fear generalization (Dunsmoor et al., 2011; Greenberg et al., 2013; Lissek et al., 2014a; Kaczkurkin et al., 2017), yet we did not replicate this effect. In the current study, the threat cue was reinforced on 100% of CS+ trials. Other studies have utilized reinforcement rates ranging from 62.5 (Dunsmoor et al., 2011) to 80% (Lissek et al., 2014a), allowing trials where the BOLD signal is contaminated by electrical stimulation to be discarded. While known to play a key role in anxious anticipation and salience detection, the insula is also critically involved in interoception and somatic processing (Grupe and Nitschke, 2013; Singer et al., 2009; Uddin et al., 2017); the defined insular fROIs, therefore, may have been reflecting perceptual response to painful stimulation and were less relevant to the generalization test.

Of course, introducing variable reinforcement schedules during acquisition adds another layer of uncertainty to the paradigm; however, switching from continuous to intermittent reinforcement between conditioning and generalization, as in the current study, may also introduce unintentional variability and ambiguity about threat contingencies. Underlying theoretical models and prior work in fear conditioning suggest that threat reinforcement rates have profound effects on learning and recall of threat contingencies (Grady et al., 2016; Wagner et al., 1967) and may be moderated by individual differences in anxiety (Chin et al., 2016; Lonsdorf and Merz, 2017). Given that uncertainty may be a key mechanism contributing to fear generalization (Hunt et al., 2019; Morriss et al., 2016; Nelson et al., 2015), it is important to understand the implications of initial threat predictability when later introducing ambiguous stimuli.

Further diverging from prior work, results of the current study revealed consistently linear – rather than quadratic – generalization effects. In both animal (Honig and Urcuioli, 1981) and human (Lissek et al., 2008) samples, quadratic gradients generally reflect an adaptive degree of generalization. Linear gradients, on the other hand, are typically observed in clinical samples (Kaczkurkin et al., 2017; Lissek et al., 2009, 2014b), consistent with behavioral phenotypes suggestive of overgeneralized threat responding in anxious pathologies (Dymond et al., 2015; Lissek et al., 2008; Lissek, 2012). The current

sample comprised healthy young adults, yet generalization gradients were more similar to those previously found in clinical samples. The reason for this is unclear. As this was a novel task, one possibility relates to the conditioned and generalization stimuli used; previous studies have typically utilized simple geometric shapes (e.g., circles (Lissek et al., 2014a; van Meurs et al., 2014)), rectangles (Cha et al., 2014; Greenberg et al., 2013), faces (Dunsmoor et al., 2011), and conceptual categories (Morey et al., 2020). Gabor patches have been used infrequently in other aversive stimulus generalization paradigms (Koban et al., 2018; McTeague et al., 2015). In the current paradigm, stimuli varied an average of 3.33° from the next most similar stimulus; this narrow difference perhaps made the task quite challenging compared to alternative stimuli or even similar stimuli with greater steps of differentiation (e.g., ± 10° (McTeague et al., 2015)). Interestingly, a study by Koban and colleagues (Koban et al., 2018) found a similar linear generalization effect for conditioned pain modulation using similar stimuli (i.e., Gabor patches varying by ± 4°). It is possible that smaller degrees of change between conditioned and generalization stimuli – considering both variation across stimuli and shared perceptual space (Aizenberg and Geffen, 2013; Chapuis and Wilson, 2011; McGann, 2015) - biases generalization gradients towards different shapes. There may also be important discrepancies of visual cortex processing, given the inherent properties of Gabor patches. Future work examining this idea in a systematic fashion would be beneficial, as it may influence how we conceptualize quadratic and linear gradients as adaptive and (potentially) pathologic, respectively.

The current study is limited in several aspects. First, the sample comprised relatively healthy, young adults. While this has allowed us to contribute to the growing literature about the neural bases of fear generalization, it has limited generalizability to other populations. In particular, given the proposed clinical relevance of threat generalization in psychiatric disorders (Dunsmoor and Paz, 2015; Dymond et al., 2015; Lissek, 2012), future translational work is critical, as there may be important clinical implications (e.g., prediction of psychopathology onset, potential treatment target). Our sample was also limited in size, leaving us underpowered to examine effects of individual differences in anxious traits, and those findings must be considered preliminary. Additionally, while partial coverage scans allowed us to optimize high spatial resolution for our small a priori regions of interest (e.g., hippocampal subfields, habenula), we were unable to examine regions previously implicated in fear generalization (e.g., dorsomedial prefrontal cortex (Kaczkurkin et al., 2017; Lissek et al., 2014a)) as they were outside of the functional scan coverage. Although use of shock expectancy ratings is common in fear conditioning and generalization work (e.g., (Morey et al., 2015)), it is possible that their inclusion could have had unintended consequences on results related to expectancies and/or demand characteristics (Sjouwerman et al., 2016). Finally, individuals vary in their low-level perceptual discrimination abilities (Ward et al., 2017). Although research suggests that generalization effects cannot be fully explained by individual differences in perceptual discriminability (Guttman and Kalish, 1956; Onat and Büchel, 2015; Tuominen et al., 2019), there may still be important effects on generalization (Dunsmoor and Paz, 2015; Struyf et al., 2015; Zaman et al., 2020). Indeed, studies have found generalization is related to perceptual errors (i.e., misclassification of generalization stimuli as the CS+; (Zaman et al., 2019)), though it remains unclear whether such errors are effects of true perceptual differences or reflect higher-order cognitive processes (e.g., memory biases; Mitte, 2008). As such, future studies would benefit from additional procedures (e.g., discrimination threshold testing) that allow for consideration of these differences in analyses.

5. Conclusions

Overall, these findings largely support previous work on the neurobiological bases of fear generalization and make a compelling case for further examination of regions (e.g., habenula, hippocampal subfields)

that have been poorly studied due to the technological constraints of standard neuroimaging parameters. Key differences (e.g., linear shaped gradients), however, suggest that our current understanding of fear generalization and its neural substrates is incomplete. Fear generalization, therefore, remains a promising area of study. In the current study, generalization to safety cues was largely uninformative, however, expanding generalization beyond threat may prove valuable in work with clinical samples, where aberrancies in safety generalization may play a unique role in the pathophysiology of these disorders. Further work is certainly warranted in order to disentangle the complexities of this process, particularly given generalization's strong clinical relevance. In fact, emerging work has shown that perceptual discrimination training can reduce avoidance behavior and decrease arousal in anxious populations (Ginat-Frolich et al., 2019; Lommen et al., 2017), suggesting generalization may be a useful, modifiable treatment target. Moving forward, it is essential to implement readily quantifiable and variable parametric space within generalization paradigms to better understand these processes and disentangle effects related to psychopathology versus perception. Keeping in mind the goal of replicability in science, it is also critical that future work employs sound methods to better ascertain how experimental conditions may influence neural response, as well as larger sample sizes to reliably detect associations with anxious traits. Being able to better link behavioral and clinical phenotypes to the brain's function is certain to provide further insight that will aid in developing and optimizing effective treatments.

Data and code availability statement

The data for the attached paper entitled "Neural substrates of fear generalization: A 7T-fMRI investigation" are not currently available for sharing based upon institutional restrictions. However, we are exploring potential availability and sharing options with the University of Wisconsin—Milwaukee and Medical College of Wisconsin Institutional Review Boards. We welcome inquests regarding data availability other correspondence about this article. We can be reached via email at huggins@uwm.edu or larsoncl@uwm.edu.

Supplementary materials

Supplementary material associated with this article can be found, in the online version, at doi:10.1016/j.neuroimage.2021.118308.

Credit authorship contribution statement

Ashley A. Huggins: Conceptualization, Methodology, Formal analysis, Writing – original draft, Writing – review & editing, Visualization. **Carissa N. Weis:** Formal analysis, Writing – review & editing, Investigation. **Elizabeth A. Parisi:** Writing – review & editing, Investigation. **Kenneth P. Bennett:** Writing – review & editing, Investigation. **Vladimir Miskovic:** Writing – review & editing, Methodology, Supervision. **Christine L. Larson:** Funding acquisition, Conceptualization, Methodology, Project administration, Writing – review & editing.

References

Ahrens, L.M., Pauli, P., Reif, A., Mühlberger, A., Langs, G., Aalderink, T., Wieser, M.J., 2016. Fear conditioning and stimulus generalization in patients with social anxiety disorder. J. Anxiety 44, 36–46. http://doi.org/10.1016/j.janxdis.2016.10.003.

Aimone, J.B., Deng, W., Gage, F.H., 2011. Resolving new memories: a critical look at the dentate gyrus, adult neurogenesis, and pattern separation. Neuron 70 (4), 589–596.

Aizenberg, M., Geffen, M.N., 2013. Bidirectional effects of aversive learning on perceptual acuity are mediated by the sensory cortex. Nat. Neurosci. 16, 994–996. doi:10.1038/nn.3443.

Alvarez, R.P., Chen, G., Bodurka, J., Kaplan, R., Grillon, C., 2011. Phasic and sustained fear in humans elicits distinct patterns of brain activity. Neuroimage 55 (1), 389–400. http://doi.org/10.1016/j.neuroimage.2010.11.057.

Amaral, D.G., Scharfman, H.E., Lavenex, P., 2007. The dentate gyrus: fundamental neuroanatomical organization (dentate gyrus for dummies). In: The Dentate Gyrus: A Comprehensive Guide to Structure, Function, and Clinical Implications. Elsevier, pp. 3–790 Vol. 163.

Armony, J.L., Dolan, R.J., 2001. Modulation of auditory neural responses by a visual context in human fear conditioning. Neuroreport 12 (15), 3407–3411.

Arnaudova, I., Krypotos, A.-.M., Effting, M., Kindt, M., Beckers, T., 2017. Fearing shades of grey: individual differences in fear responding towards generalisation stimuli. Cogn. Emot. 31 (6), 1181–1196. http://doi.org/10.1080/02699931.2016.1204990.

Asok, A., Kandel, E.R., Rayman, J.B., 2019. The neurobiology of fear generalization. Front. Behav. Neurosci. 12, 329. http://doi.org/10.3389/fnbeh.2018.00329.

Avery, S.N., Clauss, J.A., Winder, D.G., Woodward, N., Heckers, S., Blackford, J.U., 2014. BNST neurocircuitry in humans. Neuroimage 91, 311–323. http://doi.org/10.1016/j.neuroimage.2014.01.017.

Bakker, A., Kirwan, C.B., Miller, M., Stark, C.E.L., 2008. Pattern separation in the human hippocampal CA3 and dentate gyrus. Science 319 (5870), 1640–1642. http://doi.org/10.1126/science.1152882.

Barnes, L.L.B., Harp, D., Jung, W.S., 2002. Reliability generalization of scores on the Spielberger State-Trait Anxiety Inventory. Educ. Psychol. Meas. 62 (4), 603. –603 http://doi.org/10.1177/0013164012287759049 .

Bauer, E.A., MacNamara, A., Sandre, A., Lonsdorf, T.B., Weinberg, A., Morriss, J., van Reekum, C.M., 2020. Intolerance of uncertainty and threat generalization: a replication and extension. Psychophysiology 57 (5).

Berron, D., Vieweg, P., Hochkeppler, A., Pluta, J. B., Ding, S. L., Maass, A., Luther, A., Xie, L., Das, S. R., Wolk, D. A., Wolbers, T., Yushkevich, P. A., Düzel, E., Wisse, L. E. M., 2017. A protocol for manual segmentation of medial temporal lobe subregions in 7 Tesla MRI. NeuroImage Clin 15, 466–482. https://doi.org/10.1016/j.nicl.2017.05.022.

Besnard, A., Sahay, A., 2016. Adult hippocampal neurogenesis, fear generalization, and stress. Neuropsychopharmacology 41 (1), 24–44. http://doi.org/10.1038/npp.2015.167.

Boulos, L.-.J., Darcq, E., Kieffer, B.L., 2017. Translating the habenula—from rodents to humans. Biol. Psychiatry 81 (4), 296–305. http://doi.org/10.1016/j.biopsych.2016.06.003.

Brown, V.M., LaBar, K.S., Haswell, C.C., Gold, A.L., Workgroup, Mid-Atlantic MIRECC, McCarthy, G., Morey, R.A, 2014. Altered resting-state functional connectivity of basolateral and centromedial amygdala complexes in posttraumatic stress disorder. Neuropsychopharmacology 39 (2), 351–359. http://doi.org/10.1038/npp.2013.197.

Bucci, D.J., Saddoris, M.P., Burwell, R.D., 2002. Contextual fear discrimination is impaired by damage to the postrhinal or perirhinal cortex. Behav. Neurosci. 116 (3), 479–488.

Buhr, K., Dugas, M.J., 2002. The Intolerance of Uncertainty Scale: psychometric properties of the English version. Behav. Res. Ther. 40 (8), 931–945.

Cha, J., Greenberg, T., Carlson, J.M., Dedora, D.J., Hajcak, G., Mujica-Parodi, L.R., 2014. Circuit-wide structural and functional measures predict ventromedial prefrontal cortex fear generalization: implications for generalized anxiety disorder. J. Neurosci. 34 (11), 4043–4053. http://doi.org/10.1523/JNEUROSCI.3372-13.2014.

Chapuis, J., Wilson, D.A., 2011. Bidirectional plasticity of cortical pattern recognition and behavioral sensory acuity. Nat. Neurosci. 15, 155–161. doi:10.1038/nn.2966.

Chin, B., Nelson, B.D., Jackson, F., Hajcak, G., 2016. Intolerance of uncertainty and startle potentiation in relation to different threat reinforcement rates. Int. J. Psychophysiol. 99, 79–84. doi:10.1016/j.ijpsycho.2015.11.006.

Clelland, C.D., Choi, M., Romberg, C., Clemenson, G.D., Fragniere, A., Tyers, P., et al., 2009. A functional role for adult hippocampal neurogenesis in spatial pattern separation. Science 325 (5937), 210–213. http://doi.org/10.1126/science.1173215.

Correa, K.A., Liu, H., Shankman, S.A., 2019. The role of intolerance of uncertainty in current and remitted internalizing and externalizing psychopathology. J. Anxiety Disord. 62, 68–76. http://doi.org/10.1016/j.janxdis.2019.01.001.

Cox, R.W., 1996. AFNI: software for analysis and visualization of functional magnetic resonance neuroimages. Comput.Biomed. Res. 29 (3), 162–173. http://doi.org/10.1006/cbmr.1996.0014.

... Das, P., Kemp, A.H., Liddell, B.J., Brown, K.J., Olivieri, G., Peduto, A., Williams, L.M., 2005. Pathways for fear perception: modulation of amygdala activity by thalamo-cortical systems. Neuroimage 26 (1), 141–148.

Davis, M., 1992. The role of the amygdala in fear and anxiety. Annu. Rev. Neurosci. 15 (1), 353–375. http://doi.org/10.1146/annurev.ne.15.030192.002033.

Davis, M., Walker, D.L., Miles, L., Grillon, C., 2010. Phasic vs sustained fear in rats and humans: role of the extended amygdala in fear vs anxiety. Neuropsychopharmacology 35 (1), 105–135. http://doi.org/10.1038/npp.2009.109.

Dimsdale-Zucker, H.R., Ritchey, M., Ekstrom, A.D., Yonelinas, A.P., Ranganath, C., 2018. CA1 and CA3 differentially support retrieval of episodic contexts within human hippocampal subfields. Nat. Commun. 9, 294. doi:10.1038/s41467-017-02752-1.

Dugas, M.J., Gagnon, F., Ladouceur, R., Freeston, M.H., 1998. Generalized anxiety disorder: a preliminary test of a conceptual model. Behav. Res. Ther. 36 (2), 215–226.

... Duits, P., Cath, D.C., Lisek, S., Hox, J.J., Hamm, A.O., Engelhard, I.M., Baas, J.M., 2015. Updated meta-analysis of classical fear conditioning in the anxiety disorders. Depress. Anxiety 32 (4), 239–253.

Dunsmoor, J.E., Mitroff, S.R., LaBar, K.S., 2009. Generalization of conditioned fear along a dimension of increasing fear intensity. Learn. Memory 16 (7), 460–469. http://doi.org/10.1101/lm.1431609.

Dunsmoor, J. E., Paz, R., 2015. Fear generalization and anxiety: behavioral and neural mechanisms. Biol. Psychiatry 78 (5), 336–343. https://doi.org/10.1016/j.biopsych.2015.04.010.

Dunsmoor, J.E., Prince, S.E., Murty, V.P., Kragel, P.A., LaBar, K.S., 2011. Neurobehavioral mechanisms of human fear generalization. Neuroimage 55 (4), 1878–1888. http://doi.org/10.1016/j.neuroimage.2011.01.041.

Durieux, L., Mathis, V., Herbeaux, K., Muller, M., Barbelivien, A., Mathis, C., Schlichter, R., Hugel, S., Majchrzak, M., Lecourtier, L., 2020. Involvement of the lateral habenula in fear memory. Brain Struct. Funct. 225, 2029–2044. https://doi.org/10.1007/s00429-020-02107-5.

Dymond, S., Dunsmoor, J.E., Vervliet, B., Roche, B., Hermans, D., 2015. Fear general-

ization in humans: systematic review and implications for anxiety disorder research. Behav. Ther. 46 (5), 561–582. http://doi.org/10.1016/j.beth.2014.10.001.

Ely, B.A., Xu, J., Goodman, W.K., Lapidus, K.A., Gabbay, V., Stern, E.R., 2016. Resting-state functional connectivity of the human habenula in healthy individuals: associations with subclinical depression. Hum. Brain Mapp. 37 (7), 2369–2384. http://doi.org/10.1002/hbm.23179.

Epstein, E.L., Hurley, R.A., Taber, K.H., 2018. The habenula's role in adaptive behaviors: contributions from neuroimaging. J. Neuropsychiatry Clin. Neurosci. 30 (1). A4–4 http://doi.org/10.1176/appi.neuropsych.17110254 .

Etkin, A., Wager, T.D., 2007. Functional neuroimaging of anxiety: a meta-analysis of emotional processing in PTSD, social anxiety disorder, and specific phobia. Am. J. Psychiatry 164 (10), 1476–1488. http://doi.org/10.1176/appi.ajp.2007.07030504.

Ferneyhough, E., Kim, M. K., Phelps, E. A., Carrasco, M., 2013. Anxiety modulates the effects of emotion and attention on early vision. Cogn. Emot. 27 (1), 166–176. https://psycnet.apa.org/doi/10.1080/02699931.2012.689953.

Fox, A.S., Oler, J.A., Tromp, D.P.M., Fudge, J.L., Kalin, N.H., 2015. Extending the amygdala in theories of threat processing. Trends Neurosci. 38 (5), 319–329. http://doi.org/10.1016/j.tins.2015.03.002.

Freese, J.L., Amaral, D.G., 2005. The organization of projections from the amygdala to visual cortical areas TE and V1 in the macaque monkey. J. Comp. Neurol. 486 (4), 295–317.

Freeston, M. H., Rhéaume, J., Letarte, H., Dugas, M. J., Ladouceur, R., 1994. Why do people worry? Pers. Individ. Differ. 17 (6), 791–802. https://doi.org/10.1016/0191-8869(94)90048-5.

Fullana, M. A., Harrison, B. J., Soriano-Mas, C., Vervliet, B., Cardoner, N., Àvila-Parcet, A., Radua, J., 2016. Neural signatures of human fear conditioning: an updated and extended meta-analysis of fMRI studies. Mol. Psychiatry 21, 500–508. http://doi.org/10.1038/mp.2015.88.

Gazendam, F.J., Kamphuis, J.H., Kindt, M., 2013. Deficient safety learning characterizes high trait anxious individuals. Biol. Psychol. 92, 342–352.

Ginat-Frolich, R., Gendler, T., Marzan, D., Tsuk, Y., Shechner, T., 2019. Reducing fear overgeneralization in children using a novel perceptual discrimination task. Behav. Res. Ther. 116, 131–139. doi:10.1016/j.brat.2019.03.008.

Giuliano, A., Donatelli, G., Cosottini, M., Tosetti, M., Retico, A., Fantacci, M.E., 2017. Hippocampal subfields at ultra high field MRI: an overview of segmentation and measurement methods. Hippocampus 27 (5), 481–494. http://doi.org/10.1002/hipo.22717.

Glover, L.R., Schoenfeld, T.J., Karlsson, R.-.M., Bannerman, D.M., Cameron, H.A., 2017. Ongoing neurogenesis in the adult dentate gyrus mediates behavioral responses to ambiguous threat cues. PLoS Biol. 15 (4), e2001154. http://doi.org/10.1371/journal.pbio.2001154.

Goode, T.D., Ressler, R.L., Acca, G.M., Miles, O.W., & Maren, S. (2019). Bed nucleus of the stria terminalis regulates fear to unpredictable threat signals, 142, 251–62. http://doi.org/10.1101/376228

Goosens, K.A., Maren, S., 2001. Contextual and auditory fear conditioning are mediated by the lateral, basal, and central amygdaloid nuclei in rats. Learn. Memory 8 (3), 148–155. http://doi.org/10.1101/lm.37601.

Gorka, A.X., Torrisi, S., Shackman, A.J., Grillon, C., Ernst, M., 2018. Intrinsic functional connectivity of the central nucleus of the amygdala and bed nucleus of the stria terminalis. Neuroimage 168, 392–402. http://doi.org/10.1016/j.neuroimage.2017.03.007.

Grady, A.K., Bowen, K.H., Hyde, A.T., Totsch, S.K., Knight, D.C., 2016. Effect of continuous and partial reinforcement on the acquisition and extinction of human conditioned fear. Behav. Neurosci. 130 (1), 36–43.

Greenberg, T., Carlson, J.M., Cha, J., Hajcak, G., Mujica-Parodi, L.R., 2013. Neural reactivity tracks fear generalization gradients. Biol. Psychol. 92 (1), 2–8. http://doi.org/10.1016/j.biopsycho.2011.12.007.

Grosso, A., Santoni, G., Manassero, E., Renna, A., Sacchetti, B., 2018. A neuronal basis for fear discrimination in the lateral amygdala. Nat. Commun. 9 (1), 158. http://doi.org/10.1038/s41467-018-03682-2.

Grupe, D.W., Nitschke, J.B., 2013. Uncertainty and anticipation in anxiety: an integrated neurobiological and psychological perspective. Nat. Rev. Neurosci. 14 (7), 488–501. http://doi.org/10.1038/nrn3524.

Guttman, N., Kalish, H.I., 1956. Discriminability and stimulus-generalization. J. Exp. Psychol. 51, 79–88.

Guzowski, J.F., Knierim, J.J., Moser, E.I., 2004. Ensemble dynamics of hippocampal regions CA3 and CA1. Neuron 44 (4), 581–584.

Haddad, A.D.M., Xu, J., Raeder, S., Lau, J.Y.F., 2013. Measuring the role of conditioning and stimulus generalisation in common fears and worries. Cogn. Emot. 27 (5), 914–922. http://doi.org/10.1080/02699931.2012.747428.

Hanert, A., Pedersen, A., Bartsch, T., 2019. Transient hippocampal CA1 lesions in humans impair pattern separation performance. Hippocampus 29 (8), 736–747.

Hayes, J.P., Hayes, S., Miller, D.R., Lafleche, G., Logue, M.W., Verfaellie, M., 2017. Automated measurement of hippocampal subfields in PTSD: evidence for smaller dentate gyrus volume. J. Psychiatr. Res. 95, 247–252. http://doi.org/10.1016/j.jpsychires.2017.09.007.

Hennigan, K., D'Ardenne, K., McClure, S.M., 2015. Distinct midbrain and habenula pathways are involved in processing aversive events in humans. J. Neurosci. 35 (1), 198–208. http://doi.org/10.1523/JNEUROSCI.0927-14.2015.

Hikosaka, O., 2010. The habenula: from stress evasion to value-based decision-making. Nat. Rev. Neurosci. 11 (7), 503–513. http://doi.org/10.1038/nrn2866.

Honig, W. K., Urcuioli, P. J., 1981. The legacy of Guttman and Kalish (1956): 25 years of research on stimulus generalization. J. Exp. Anal. Behav. 36 (3), 405–445. http://doi.org/10.1901/jeab.1981.36-405.

Hunsaker, M.R., Kesner, R.P., 2013. The operation of pattern separation and pattern completion processes associated with different attributes or domains of memory. Neurosci. Biobehav. Rev. 37 (1), 36–58.

Hunt, C., Cooper, S.E., Hartnell, M.P., Lissek, S., 2019. Anxiety sensitivity and intolerance of uncertainty facilitate associations between generalized Pavlovian fear and maladaptive avoidance decisions. J. Abnorm. Psychol. 128 (4), 315–326. http://doi.org/10.1037/abn0000422.

... Hur, J., Smith, J.F., DeYoung, K.A., Anderson, A.S., Kuang, J., ChoKim, H., Shackman, A.J., 2020. Anxiety and the neurobiology of temporally uncertain threat anticipation. J. Neurosci. 40 (41), 7949–7964. http://doi.org/10.1523/JNEUROSCI.0704-20.2020 .

Janak, P.H., Tye, K.M., 2015. From circuits to behaviour in the amygdala. Nature 517 (7534), 284–292. http://doi.org/10.1038/nature14188.

Kaczkurkin, A.N., Burton, P.C., Chazin, S.M., Manbeck, A.B., Espensen-Sturges, T., Cooper, S.E., et al., 2017. Neural Substrates of Overgeneralized Conditioned Fear in PTSD. Am. J. Psychiatry 174 (2), 125–134. http://doi.org/10.1176/appi.ajp.2016.15121549.

Kheirbek, M.A., Klemenhagen, K.C., Sahay, A., Hen, R., 2012. Neurogenesis and generalization: a new approach to stratify and treat anxiety disorders. Nat. Neurosci. 15 (12), 1613–1620. http://doi.org/10.1038/nn.3262.

Klumpers, F., Kroes, M.C.W., Baas, J., Fernández, G., 2017. How human amygdala and bed nucleus of the stria terminalis may drive distinct defensive responses. J. Neurosci. 3830. –16 http://doi.org/10.1523/JNEUROSCI.3830-16.2017 .

Koban, L., Kusko, D., Wager, T.D., 2018. Generalization of learned pain modulation depends on explicit learning. Acta Psychol. 184, 75–84. doi:10.1016/j.actpsy.2017.09.009.

Lacy, J.W., Yassa, M.A., Stark, S.M., Muftuler, L.T., Stark, C.E.L., 2011. Distinct pattern separation related transfer functions in human CA3/dentate and CA1 revealed using high-resolution fMRI and variable mnemonic similarity. Learn. Mem. 18 (1), 15–18. doi:10.1101/lm.1971111.

Ladouceur, R., Gosselin, P., Dugas, M.J., 2000. Experimental manipulation of intolerance of uncertainty: a study of a theoretical model of worry. Behav. Res. Ther. 38 (9), 933–941.

... Lange, I., Goossens, L., Bakker, J., Michielse, S., van Winkel, R., Lissek, S., Schruers, K., 2019. Neurobehavioural mechanisms of threat generalization moderate the link between childhood maltreatment and psychopathology in emerging adulthood. J. Psychiatry Neurosci. 44 (3), 185–194. doi:10.1503/jpn.180053.

Lawson, R.P., Drevets, W.C., Roiser, J.P., 2013. Defining the habenula in human neuroimaging studies. Neuroimage 64, 722–727. http://doi.org/10.1016/j.neuroimage.2012.08.076.

Lawson, R.P., Nord, C.L., Seymour, B., Thomas, D.L., Dayan, P., Pilling, S., Roiser, J.P., 2017. Disrupted habenula function in major depression. Mol. Psychiatry 22 (2), 202–208. http://doi.org/10.1038/mp.2016.81.

Lebow, M.A., Chen, A., 2016. Overshadowed by the amygdala: the bed nucleus of the stria terminalis emerges as key to psychiatric disorders. Mol. Psychiatry 21 (4), 450–463. http://doi.org/10.1038/mp.2016.1.

LeDoux, J., 2003. The emotional brain, fear, and the amygdala. Cell. Mol. Neurobiol. 23 (4–5), 727–738.

... Lis, S., Thome, J., Kleindienst, N., Mueller-Engelmann, M., Steil, R., Priebe, K., Bohus, M., 2020. Generalization of fear in post-traumatic stress disorder. Psychophysiology 57, e13422. doi:10.1111/psyp.13422.

Lissek, S., 2012. Toward an account of clinical anxiety predicated on basic, neurally mapped mechanisms of Pavlovian fear-learning: the case for conditioned overgeneralization. Depress. Anxiety.

Lissek, S., van Meurs, B., 2015. Learning models of PTSD: theoretical accounts and psychobiological evidence. Int. J. Psychophysiol. 98 (3), 594–605. http://doi.org/10.1016/j.ijpsycho.2014.11.006.

Lissek, S., Biggs, A.L., Rabin, S.J., Cornwell, B.R., Alvarez, R.P., Pine, D.S., Grillon, C., 2008. Generalization of conditioned fear-potentiated startle in humans: experimental validation and clinical relevance. Behav. Res. Ther. 46 (5), 678–687. http://doi.org/10.1016/j.brat.2008.02.005.

Lissek, S., Bradford, D.E., Alvarez, R.P., Burton, P., Espensen-Sturges, T., Reynolds, R.C., Grillon, C., 2014a. Neural substrates of classically conditioned fear-generalization in humans: a parametric fMRI study. Soc Cogn Affect Neurosci 9 (8), 1134–1142. http://doi.org/10.1093/scan/nst096.

Lissek, S., Kaczkurkin, A.N., Rabin, S., Geraci, M., Pine, D.S., Grillon, C., 2014b. Generalized Anxiety Disorder Is Associated With Overgeneralization of Classically Conditioned Fear. Biol. Psychiatry 75 (11), 909–915. http://doi.org/10.1016/j.biopsych.2013.07.025.

Lissek, S., Rabin, S., Heller, R.E., 2009. Overgeneralization of conditioned fear as a pathogenic marker of panic disorder. Am. J. Psychiatry.

Lommen, M.J.J., Duta, M., Vanbrabant, K., de Jong, R., Juechems, K., Ehlers, A., 2017. Training discrimination diminishes maladaptive avoidance of innocuous stimuli in a fear conditioning paradigm. PLoS One 12 (10), e0184485.

Lonsdorf, T. B., Klingelhöfer-Jens, M., Andreatta, M., Beckers, T., Chalkia, A., Gerlicher, A., Jentsch, V. L., Drexler, S. M., Mertens, G., 2019. Navigating the garden of forking paths for data exclusions in fear conditioning research. eLife 8, e52465. https://doi.org/10.7554/eLife.52465.

Lonsdorf, T.B., Merz, C.J., 2017. More than just noise: inter-individual differences in fear acquisition, extinction and return of fear in humans-Biological, experiential, temperamental factors, and methodological pitfalls. Neurosci. Biobehav. Rev. 80, 703–728.

Mathuru, A.S., Jesuthasan, S., 2013. The medial habenula as a regulator of anxiety in adult zebrafish. Front Neural Circ. 7, 99. http://doi.org/10.3389/fncir.2013.00099.

Matsumoto, M., Hikosaka, O., 2007. Lateral habenula as a source of negative reward signals in dopamine neurons. Nature 447 (7148), 1111–1115. http://doi.org/10.1038/nature05860.

McGann, J.P., 2015. Associative learning and sensory neuroplasticity: how does it happen and what is it good for? Learn. Memory 22, 567–576 doi.org/10.1101/lm.039636.115.

McHugh, T.J., Jones, M.W., Quinn, J.J., Balthasar, N., Coppari, R., Elmquist, J.K., et al., 2007. Dentate gyrus NMDA receptors mediate rapid pattern separation in the hippocampal network. Science 317 (5834), 94–99. http://doi.org/10.1126/science.1140263.

McTeague, L.M., Gruss, L.F., Keil, A., 2015. Aversive learning shapes neuronal orientation tuning in human visual cortex. Nat. Commun. 6, 7823.

Miskovic, V., Keil, A., 2012. Acquired fears reflected in cortical sensory processing: a review of electrophysiological studies of human classical conditioning. Psychophysiology 49 (9), 1230–1241.

Miskovic, V., Keil, A., 2013. Visuocortical changes during delay and trace aversive conditioning: evidence from steady-state visual evoked potentials. Emotion 13 (3), 554–561. doi:10.1037/a0031323.

Mitte, K., 2008. Memory bias for threatening information in anxiety and anxiety disorders: a meta-analytic review. Psychol. Bull. 134 (6), 886–911. doi:10.1037/a0013343.

Morey, R.A., Haswell, C.C., Stjepanovic, D., Workgroup, Mid-Atlantic MIRECC, Dunsmoor, J.E., LaBar, K.S, 2020. Neural correlates of conceptual-level fear generalization in posttraumatic stress disorder. Neuropsychopharmacology 1–10.

Morey, R.A., Dunsmoor, J.E., Haswell, C.C., Brown, V.M., Vora, A., Weiner, J., Stjepanovic, D., Brancu, M., et al., 2015. Fear learning circuitry is biased toward generalization of fear associations in posttraumatic stress disorder. Transl. Psychiatry 5 (12), e700. http://doi.org/10.1038/tp.2015.196.

Morriss, J., Macdonald, B., van Reekum, C.M., 2016. What is going on around here? Intolerance of uncertainty predicts threat generalization. PLoS One 11 (5), e0154494. http://doi.org/10.1371/journal.pone.0154494.

Nelson, B.D., Weinberg, A., Pawluk, J., Gawlowska, M., Proudfit, G.H., 2015. An event-related potential investigation of fear generalization and intolerance of uncertainty. Behav Ther 46 (5), 661–670. http://doi.org/10.1016/j.beth.2014.09.010.

Onat, S., Büchel, C., 2015. The neuronal basis of fear generalization in humans. Nat. Neurosci. 18 (12), 1811–1818. https://doi.org/10.1038/nn.4166.

Osmanağaoğlu, N., Creswell, C., Dodd, H.F., 2018. Intolerance of Uncertainty, anxiety, and worry in children and adolescents: a meta-analysis. J. Affect. Disord. 225, 80–90. http://doi.org/10.1016/j.jad.2017.07.035.

Pessoa, L., Adolphs, R., 2010. Emotion processing and the amygdala: from a 'low road' to 'many roads' of evaluating biological significance. Nat. Rev. Neurosci. 11 (11), 773–783. doi:10.1038/nrn2920.

Pobbe, R.L.H., Zangrossi, H., 2008. Involvement of the lateral habenula in the regulation of generalized anxiety- and panic-related defensive responses in rats. Life Sci. 82 (25–26), 1256–1261. http://doi.org/10.1016/j.lfs.2008.04.012.

Resnik, J., Paz, R., 2015. Fear generalization in the primate amygdala. Nat. Neurosci. 18 (2), 188–190. http://doi.org/10.1038/nn.3900.

Rolls, E.T., 2013. The mechanisms for pattern completion and pattern separation in the hippocampus. Front. Syst. Neurosci. 7, 74. http://doi.org/10.3389/fnsys.2013.00074.

Salas, R., Baldwin, P., de Biasi, M., Montague, P.R., 2010. BOLD responses to negative reward prediction errors in human habenula. Front. Hum. Neurosci. 4, 36. http://doi.org/10.3389/fnhum.2010.00036.

Sarinopoulos, I., Grupe, D.W., Mackiewicz, K.L., Herrington, J.D., Lor, M., Steege, E.E., Nitschke, J.B., 2010. Uncertainty during anticipation modulates neural responses to aversion in human insula and amygdala. Cereb. Cortex 20 (4), 929–940. http://doi.org/10.1093/cercor/bhp155.

Saygin, Z.M., Kliemann, D., Iglesias, J.E., van der Kouwe, A.J.W., Boyd, E., Reuter, M., et al., 2017. High-resolution magnetic resonance imaging reveals nuclei of the human amygdala: manual segmentation to automatic atlas. Neuroimage 155, 370–382. http://doi.org/10.1016/j.neuroimage.2017.04.046.

Sep, M.S.C., Steenmeijer, A., Kennis, M., 2019. The relation between anxious personality traits and fear generalization in healthy subjects: a systematic review and meta-analysis. Neurosci. Biobehav. Rev. 107, 320–328. doi:10.1016/j.neubiorev.2019.09.029.

Sexton, K.A., Dugas, M.J., 2009. Defining distinct negative beliefs about uncertainty: validating the factor structure of the Intolerance of Uncertainty Scale. Psychol. Assess. 21 (2), 176–186. http://doi.org/10.1037/a0015827.

Shackman, A.J., Fox, A.S., 2016. Contributions of the central extended amygdala to fear and anxiety. J. Neurosci. 36 (31), 8050–8063. http://doi.org/10.1523/JNEUROSCI.0982-16.2016.

Shankman, S.A., Gorka, S.M., Nelson, B.D., Fitzgerald, D.A., Phan, K.L., O'Daly, O, 2014. Anterior insula responds to temporally unpredictable aversiveness: an fMRI study. Neuroreport 25 (8), 596–600. http://doi.org/10.1097/WNR.0000000000000144.

Shelton, L., Becerra, L., Borsook, D., 2012. Unmasking the mysteries of the habenula in pain and analgesia. Prog. Neurobiol. 96 (2), 208–219. http://doi.org/10.1016/j.pneurobio.2012.01.004.

Shi, C., Davis, M., 2001. Visual pathways involved in fear conditioning measured with fear-potentiated startle: behavioral and anatomic studies. J. Neurosci. 21 (24), 9844–9855.

Shihata, S., McEvoy, P.M., Mullan, B.A., Carleton, R.N., 2016. Intolerance of uncertainty in emotional disorders: what uncertainties remain? J. Anxiety Disord. 41, 115–124. http://doi.org/10.1016/j.janxdis.2016.05.001.

Simmons, A., Matthews, S. C., Paulus, M. P., Stein, M. B., 2008. Intolerance of uncertainty correlates with insula activation during affective ambiguity. Neurosci. Lett. 430 (2), 92–97 https://dx.doi.org/10.1016%2Fj.neulet.2007.10.030.

Singer, T., Critchley, H. D., Preuschoff, K., 2009. A common role of insula in feelings, empathy and uncertainty. Trends Cogn. Sci. 13 (8), 334–340. https://doi.org/10.1016/j.tics.2009.05.001.

Sjouwerman, R., Niehaus, J., Kuhn, M., Lonsdorf, T. B., 2016. Don't startle me - interference of startle probe presentations and intermittent ratings with fear acquisition. Psychophysiology 53 (12), 1889–1899. https://doi.org/10.1111/psyp.12761.

Solomon, P.R., Moore, J.W., 1975. Latent inhibition and stimulus generalization of the classically conditioned nictitating membrane response in rabbits (Oryctolagus cu-

niculus) following dorsal hippocampal ablation. J. Comp. Physiol. Psychol. 89 (10), 1192–1203.

Somerville, L.H., Whalen, P.J., Kelley, W.M., 2010. Human bed nucleus of the stria terminalis indexes hypervigilant threat monitoring. Biol. Psychiatry 68 (5), 416–424. http://doi.org/10.1016/j.biopsych.2010.04.002.

Spalding, K.N., 2018. The role of the medial prefrontal cortex in the generalization of conditioned fear. Neuropsychology 32 (1), 1–17. http://doi.org/10.1037/neu0000384.

Spielberger, C.D. (1983). State-Trait Anxiety Inventory for Adults. http://doi.org/10.1037/t06496-000

... Stegmann, Y., Schiele, M.A., Schümann, D., Lonsdorf, T.B., Zwanzger, P., Romanos, M., Puali, P., 2019. Individual differences in human fear generalization – pattern identification and implications for anxiety disorders. Transl. Psychiatry 9, 307. doi:10.1038/s41398-019-0646-8.

Stegmann, Y., Ahrens, L., Pauli, P., Keil, A., Wieser, M. J., 2020. Social aversive generalization sharpens the tuning of visuocortical neurons to facial identity cues. eLife 9, e55204. https://doi.org/10.7554/eLife.55204.

Strange, B.A., Fletcher, P.C., Henson, R.N., Friston, K.J., Dolan, R.J., 1999. Segregating the functions of human hippocampus. Proc. Natl. Acad. Sci. 96 (7), 4034–4039. http://doi.org/10.1073/pnas.96.7.4034.

Struyf, D., Zaman, J., Vervliet, B., Van Diest, I., 2015. Perceptual discrimination in fear generalization: mechanistic and clinical implications. Neurosci. Biobehav. Rev. 59, 201–207. doi:10.1016/j.neubiorev.2015.11.004.

Tanovic, E., Gee, D.G., Joormann, J., 2018. Intolerance of uncertainty: neural and psychophysiological correlates of the perception of uncertainty as threatening. Clin. Psychol. Rev. 60, 87–99. http://doi.org/10.1016/j.cpr.2018.01.001.

Theiss, J. D., Ridgewell, C., McHugo, M., Heckers, S., Blackford, J. U., 2017. Manual segmentation of the human bed nucleus of the stria terminalis using 3T MRI. Neuroimage 146, 288–292. https://doi.org/10.1016/j.neuroimage.2016.11.047.

Thome, J., Hauschild, S., Koppe, G., Liebke, L., Rausch, S., Herzog, J.I., et al., 2018. Generalisation of fear in PTSD related to prolonged childhood maltreatment: an experimental study. Psychol. Med. 48 (13), 2223–2234. http://doi.org/10.1017/S0033291717003713.

Tillman, R.M., Stockbridge, M.D., Nacewicz, B.M., Torrisi, S., Fox, A.S., Smith, J.F., Shackman, A.J., 2018. Intrinsic functional connectivity of the central extended amygdala. Hum. Brain Mapp. 39 (3), 1291–1312. http://doi.org/10.1002/hbm.23917.

Torrents-Rodas, D., Fullana, M.A., Bonillo, A., Caseras, X., Andión, O., Torrubia, R., 2013. No effect of trait anxiety on differential fear conditioning or fear generalization. Biol. Psychol. 92 (2), 185–190. http://doi.org/10.1016/j.biopsycho.2012.10.006.

Torrisi, S., Gorka, A.X., Gonzalez-Castillo, J., O'Connell, K., Balderston, N., Grillon, C., Ernst, M., 2018. Extended amygdala connectivity changes during sustained shock anticipation. Transl Psychiatry 8 (1), 33. http://doi.org/10.1038/s41398-017-0074-6.

Torrisi, S., Nord, C.L., Balderston, N.L., Roiser, J.P., Grillon, C., Ernst, M., 2017. Resting state connectivity of the human habenula at ultra-high field. Neuroimage 147, 872–879. http://doi.org/10.1016/j.neuroimage.2016.10.034.

Torrisi, S., O'Connell, K., Davis, A., Reynolds, R., Balderston, N., Fudge, J.L., et al., 2015. Resting state connectivity of the bed nucleus of the stria terminalis at ultra-high field. Hum. Brain Mapp. 36 (10), 4076–4088. http://doi.org/10.1002/hbm.22899.

... Tuominen, L., Boeke, E., DeCross, S., Wolthusen, R.P.F., Nasr, S., Milad, M., Holt, D., 2019. The relationship of perceptual discrimination to neural mechanisms of fear generalization. Neuroimage 188, 445–455. doi:10.1016/j.neuroimage.2018.12.034.

Tyszka, J.M., Pauli, W.M., 2016. In vivo delineation of subdivisions of the human amygdaloid complex in a high-resolution group template. Hum. Brain. Mapp. 37 (11), 3979–3998. http://doi.org/10.1002/hbm.23289.

Uddin, L. Q., Nomi, J. S., Hébert-Seropian, B., Ghaziri, J., Boucher, O., 2017. Structure and function of the human insula. J. Clin. Neurophysiol. 34 (4), 300–306. https://doi.org/10.1097/wnp.0000000000000377.

van Meurs, B., Wiggert, N., Wicker, I., Lissek, S., 2014. Maladaptive behavioral consequences of conditioned fear-generalization: a pronounced, yet sparsely studied, feature of anxiety pathology. Behav. Res. Ther. 57, 29–37. https://doi.org/10.1016/j.brat.2014.03.009.

Vuilleumier, P., Driver, J., 2007. Modulation of visual processing by attention and emotion: windows on causal interactions between human brain regions. Philos. Trans. R. Soc. B 362 (1481), 837–855.

Wagner, A.R., Siegel, L.S., Fein, G.G., 1967. Extinction of conditioned fear as a function of percentage of reinforcement. J. Comp. Psychol. 63 (1), 160–164. doi:10.1037/h0024172.

Wang, Z., Neylan, T.C., Mueller, S.G., Lenoci, M., Truran, D., Marmar, C.R., et al., 2010. Magnetic resonance imaging of hippocampal subfields in posttraumatic stress disorder. Arch. Gen. Psychiatry 67 (3), 296–303. http://doi.org/10.1001/archgenpsychiatry.2009.205.

Ward, J., Rothen, N., Chang, A., Kanai, R., 2017. The structure of inter-individual differences in visual ability: evidence from the general population and synaesthesia. Vis. Res. 141, 293–302. doi:10.1016/j.visres.2016.06.009.

Weis, C.N., Huggins, A.A., Bennett, K.P., Parisi, E.A., Larson, C.L., 2019. High-resolution resting-state functional connectivity of the extended amygdala. Brain Connect 9 (8), 627–637.

Wild, J.M., Blampied, N.M., 1972. Hippocampal lesions and stimulus generalization in rats. Physiol. Behav. 9 (4), 505–511.

Wong, A.H.K., Lovibond, P.F., 2018. Excessive generalisation of conditioned fear in trait anxious individuals under ambiguity. Behav. Res. Ther. 107, 53–63. http://doi.org/10.1016/j.brat.2018.05.012.

Yassa, M.A., Stark, C.E.L., 2011. Pattern separation in the hippocampus. Trends Neurosci. 34 (10), 515–525. http://doi.org/10.1016/j.tins.2011.06.006.

Yassa, M.A., Hazlett, R.L., Stark, C.E.L., Hoehn-Saric, R., 2012. Functional MRI of the amygdala and bed nucleus of the stria terminalis during conditions of un-

certainty in generalized anxiety disorder. J. Psychiatr. Res. 46 (8), 1045–1052. http://doi.org/10.1016/j.jpsychires.2012.04.013.

Yoshino, A., Aizawa, H., Takamura, M., Ichikawa, N., Shibasaki, C., Yamawaki, Y., et al., 2018. The role of the habenula in depression: a review of the human fMRI studies. Brain Nerve. 70 (9), 1017–1023. http://doi.org/10.11477/mf.1416201121.

Zaman, J., Struyf, D., Ceulemans, E., Vervliet, B., Beckers, T., 2020. Perceptual errors are related to shifts in generalization of conditioned responding. Psychol. Res. 1–13.

Zaman, J., Ceulemans, E., Hermans, D., Beckers, T., 2019. Direct and indirect effects of perception on generalization gradients. Behav. Res. Ther. 114, 44–50. https://doi.org/10.1016/j.brat.2019.01.006.

Zimmerman, J.M., Rabinak, C.A., McLachlan, I.G., Maren, S., 2007. The central nucleus of the amygdala is essential for acquiring and expressing conditional fear after over-training. Learn. Mem. 14 (9), 634–644. http://doi.org/10.1101/lm.607207.